Journal of Natural Gas Science and Engineering 27 (2015) 558–577

Contents lists available at ScienceDirect

Journal of Natural Gas Science and Engineering

journal homepage: www.elsevier.com/locate/jngse

Sweet spot identification in underexplored shales using multidisciplinary reservoir characterization and key performance indicators: Example of the Posidonia Shale Formation in the Netherlands☆

Jan Ter Heege [a, *], Mart Zijp [a], Susanne Nelskamp [a], Lisanne Douma [a, c, 1], Roel Verreussel [a], Johan Ten Veen [b], Geert de Bruin [a], Rene Peters [d]

[a] TNO Petroleum Geosciences, Princetonlaan 6, 3584 CB Utrecht, The Netherlands
[b] TNO Geomodelling & Geological Survey of the Netherlands, Princetonlaan 6, 3584 CB Utrecht, The Netherlands
[c] Department of Earth Sciences, Utrecht University, Budapestlaan 4, 3584 CD Utrecht, The Netherlands
[d] TNO Geo Energy, Stieltjesweg 1, Delft, The Netherlands

ARTICLE INFO

Article history:
Received 12 June 2015
Received in revised form
11 August 2015
Accepted 14 August 2015
Available online 29 August 2015

Keywords:
Sweet spot identification
Key performance indicators
Underexplored shale basins
Posidonia shale formation
North American shales
Hydrocarbon potential

ABSTRACT

Sweet spot identification in underexplored shale gas basins needs to be based on a limited amount of data on shale properties in combination with upfront geological characterization and modelling, because actual production data is usually absent. Multidisciplinary reservoir characterization and integration of modelling approaches can aid initial site selection for exploratory drilling and de-risk exploration efforts. In this study, the potential of hydrocarbon production across underexplored shale basins is analyzed using key performance indicators. A mean indicator is defined as the harmonic mean of three performance indicators that describe the potential for hydrocarbon generation, storage, and flow stimulation. The performance indicators are based on a limited number of local shale properties, i.e. vitrinite reflectance, porosity, depth, thickness, sorbed gas content and brittleness index. Values for the indicators are calculated relative to prospective North American shales (Marcellus, Bakken, Haynesville and Barnett), so that the mean indicator can be used to rank the prospectivity of an underexplored shale relative to hydrocarbon producing shales. The mean performance indicator is also used to map out the potential for gas production in the underexplored Posidonia Shale Formation in the West Netherlands Basin. The analysis shows that the performance indicator is lower for the Posidonia than for the North American Shales, mainly due to low maturity and brittleness. Local maxima of the indicator correlate with local maxima in vitrinite reflectance and depth. Besides the low potential for flow stimulation, the potential for hydrocarbon generation and storage capacity of the Posidonia are comparable to oil-window thermal-maturity Barnett Shale. Upfront simulations of hydraulic fracture properties and gas production in the Posidonia Shale Formation are in rough agreement with observed average gas flow for Barnett wells in non-core areas that are oil mature. It shows that key performance indicators can be applied to underexplored shales to quantify prospectivity and map out sweet spots across shale basins.

© 2015 Elsevier B.V. All rights reserved.

1. Introduction

North America has more than compensated the declining production of conventional hydrocarbons by the exploitation of tight and unconventional gas fields (e.g., EIA, 2015a,b). While a long track record of successful hydraulic fracturing and hydrocarbon production from shales exists in the United States (Economides and Nolte, 2000; King, 2010), such a record is lacking in many underexplored shale basins worldwide. In underexplored shale basins,

☆ Revised manuscript, submitted to Journal of Natural Gas Science and Engineering, Special issue on Advances in Practical Shale Assessment Techniques.

* Corresponding author.
E-mail addresses: jan.terheege@tno.nl (J. Ter Heege), mart.zijp@tno.nl (M. Zijp), susanne.nelskamp@tno.nl (S. Nelskamp), l.a.n.r.douma@students.uu.nl (L. Douma), roel.verreussel@tno.nl (R. Verreussel), johan.tenveen@tno.nl (J. Ten Veen), geert.debruin@tno.nl (G. de Bruin), rene.peters@tno.nl (R. Peters).
[1] Now at: Department of Geosciences & Engineering, TU Delft, Stevinweg 1, 2628 CN Delft, the Netherlands.

http://dx.doi.org/10.1016/j.jngse.2015.08.032
1875-5100/© 2015 Elsevier B.V. All rights reserved.

mapping of reservoir properties and identification of sweet spots for oil and gas production needs to be based on upfront geological characterization and modelling, i.e. before large scale exploitation has commenced. As limited data is usually available in these basins, site selection for exploratory drilling is subject to many uncertainties that can only be reduced if multidisciplinary reservoir characterization and modelling approaches are integrated (Jarvie et al., 2007; Hartwig and Schulz, 2010; Sondergeld et al., 2010; Bust et al., 2013; Verreussel et al., 2013).

Upfront geological assessment of hydrocarbon prospectivity and sweet spot identification for shales is generally performed by analyzing (1) local geological setting (e.g., burial depth, thickness, lateral distribution and fracture distribution), (2) shale composition (e.g., type and abundancy of organic matter, clay mineralogy and mineral phases in the shale matrix), and (3) shale properties (e.g., thermal maturity, porosity, permeability and brittleness). These types of analysis provide interrelated shale properties that together determine the potential of hydrocarbon production (i.e. thermal maturity is the combined effect of the abundancy and type of organic matter present and burial history). Some of the properties are used as prime indicators for hydrocarbon prospectivity of shales. The most prominent ones include total organic carbon content, vitrinite reflectance, porosity and brittleness. Total organic carbon (*TOC*) is generally used as an indicator of source rock potential. Vitrinite reflectance is generally used as an indicator of thermal maturity, which, in combination with *TOC* indicates the potential for hydrocarbon generation (Jarvie et al., 2007; Hartwig and Schulz, 2010; Van Bergen et al., 2013). Porosity is generally used together with the areal extent, thickness, hydrocarbon saturation and a depth-dependent hydrocarbon expansion factor to estimate the potentially available hydrocarbon resource of the shale play (EIA, 2011; Van Bergen et al., 2013). Preliminary predictions of the potential to fracture the shale are generally based on brittleness index (Jarvie et al., 2007; Rickman et al., 2008; Yang et al., 2013). Other properties, such as permeability, free and sorbed gas content, and reservoir pressure, are key input parameters in simulations of hydraulic fracturing and hydrocarbon production (Economides and Nolte, 2000; Godderij et al., 2014; Ter Heege et al., 2014a), but accurate analysis of these properties is generally unavailable for upfront screening of shale prospectivity. Ranges in shale properties of producing shales can be used to define screening criteria that can be compared to properties of underexplored shales to indicate prospectivity (Wang and Gale, 2009; Van Bergen et al., 2013). These indicators rely on (1) well log interpretation to derive properties such as total organic content, porosity and dynamic elastic moduli, (2) analysis of available core plugs to determine properties such as total organic content, porosity, mineralogy and brittleness, and (3) basin modelling to map out maturity and porosity across the basin. The properties from core analysis are important for calibrating properties from well log interpretation and basin modelling (Passey et al., 2010; Van Bergen et al., 2013; Crain and Holgate, 2014). The prospectivity of a shale play critically depends on the combination of the potential for hydrocarbon generation, the potential for hydrocarbon storage and the potential for flow stimulation. Poor potential for one of these processes may yield poor prospectivity of the shale as a whole. In

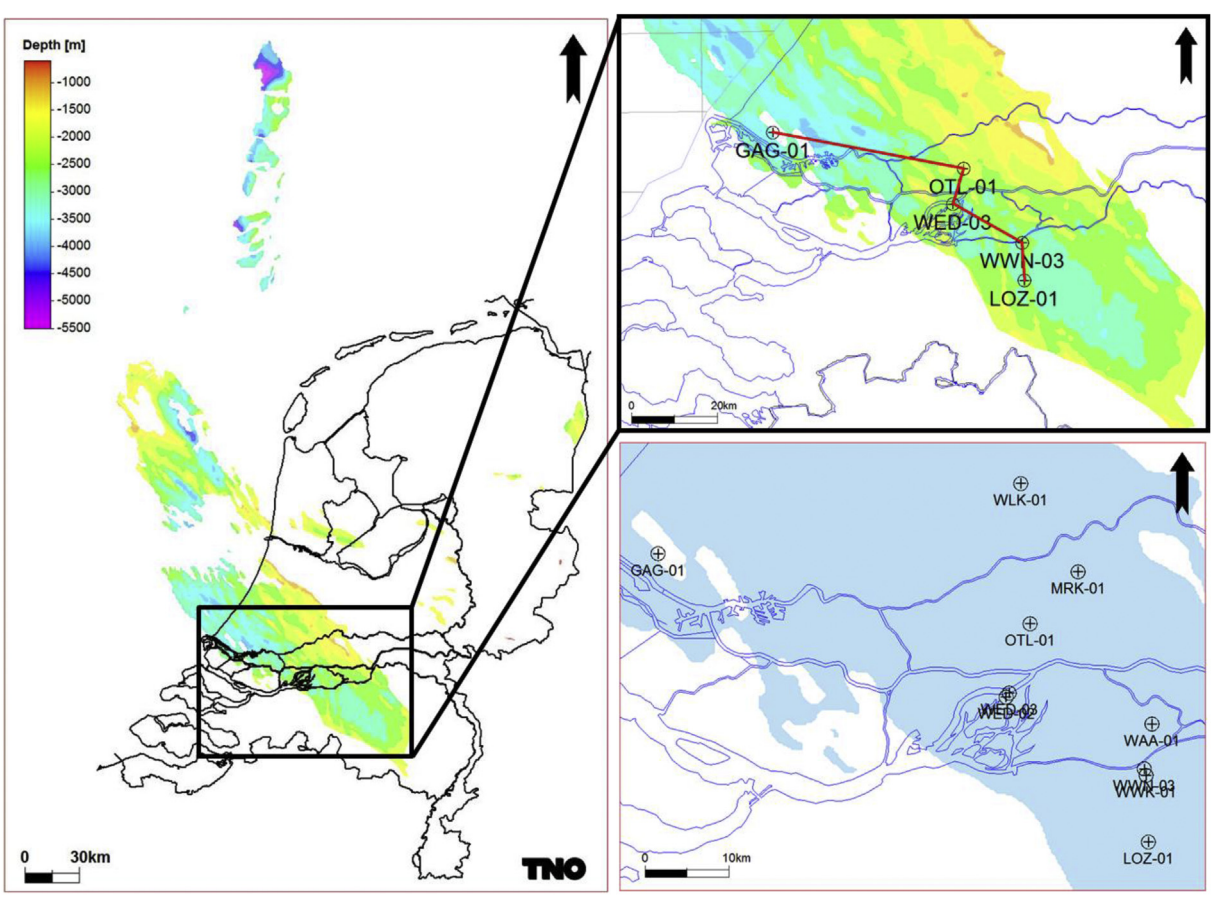

Fig. 1. Distribution and depth of the Early Jurassic Posidonia Shale Formation in the Netherlands with study area, trajectory of well log correlation (c.f. Fig. 3), and locations of all wells used in the present study.

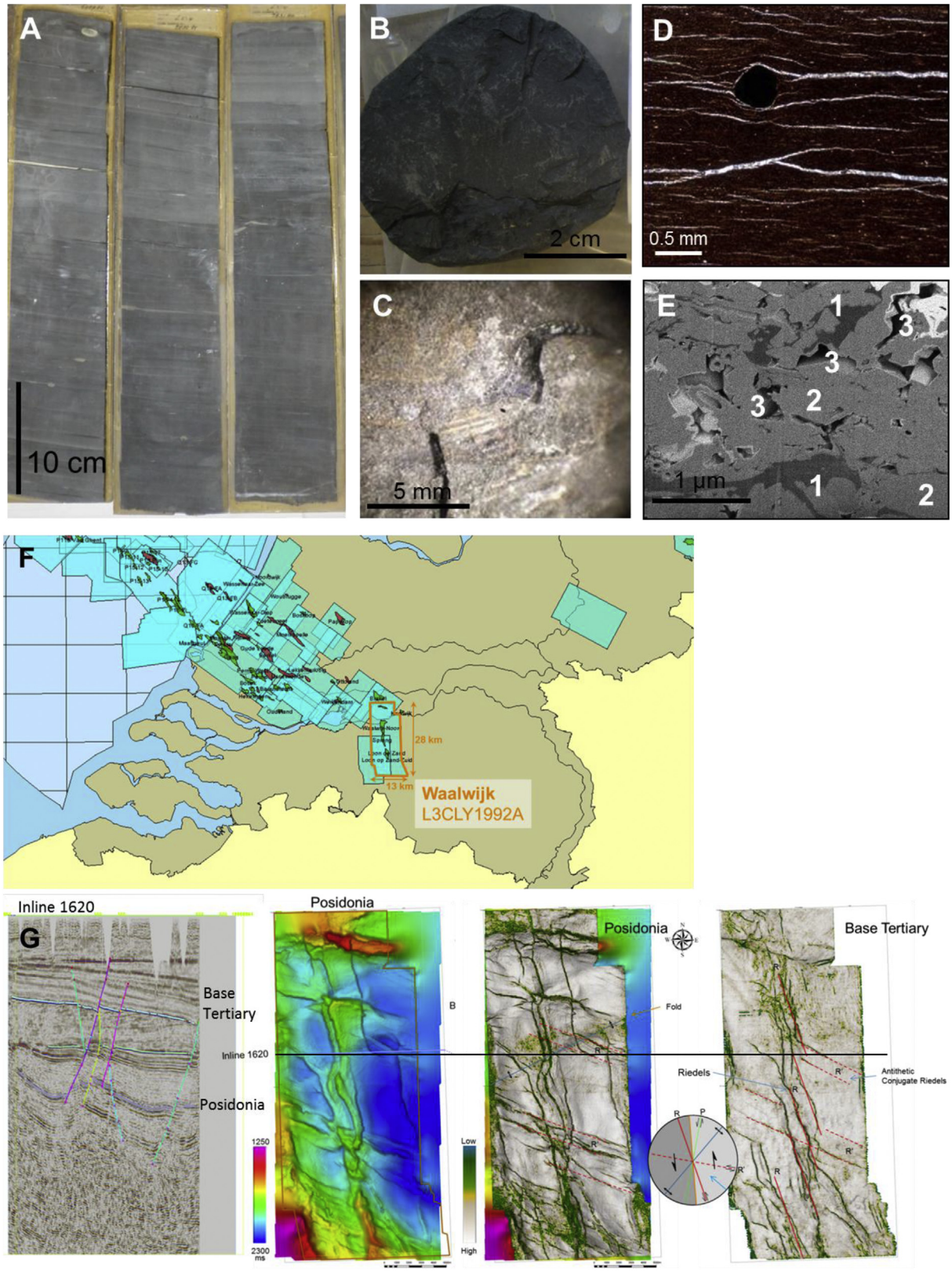

Fig. 2. The Posidonia Shale Formation from small to large scale. (A) Available core slabs. (B) Hand sized sample. (C) Centimeter scale sample with a fossilized cephalopod arm hook. (D) Light microscopy image (sample depth MD = 2491.7) showing clay minerals, calcite-filled fractures, and pyrite inclusions. (E) FIB-SEM picture (sample depth MD = 2491 m) showing the distribution of organic matter (dark grey, 1), shale matrix (light gray, 2) and porosity (black, 3). (F) Location of 3D seismic surveys including the Waalwijk (L3CLY1992A) survey used for structural analysis. (G, *from left to right*) Seismic interpretation and structural analysis of Waalwijk survey showing a vertical section with main horizons and faults (inline 1620), a time map (blue to pink indicates deeper to shallower depth), similarity (coherence, variance) attributes, and structural analysis ("Riedels") of main faults at the depth of the Posidonia Shale Formation and Base Tertiary. (For interpretation of the references to colour in this figure legend, the reader is referred to the web version of this article.)

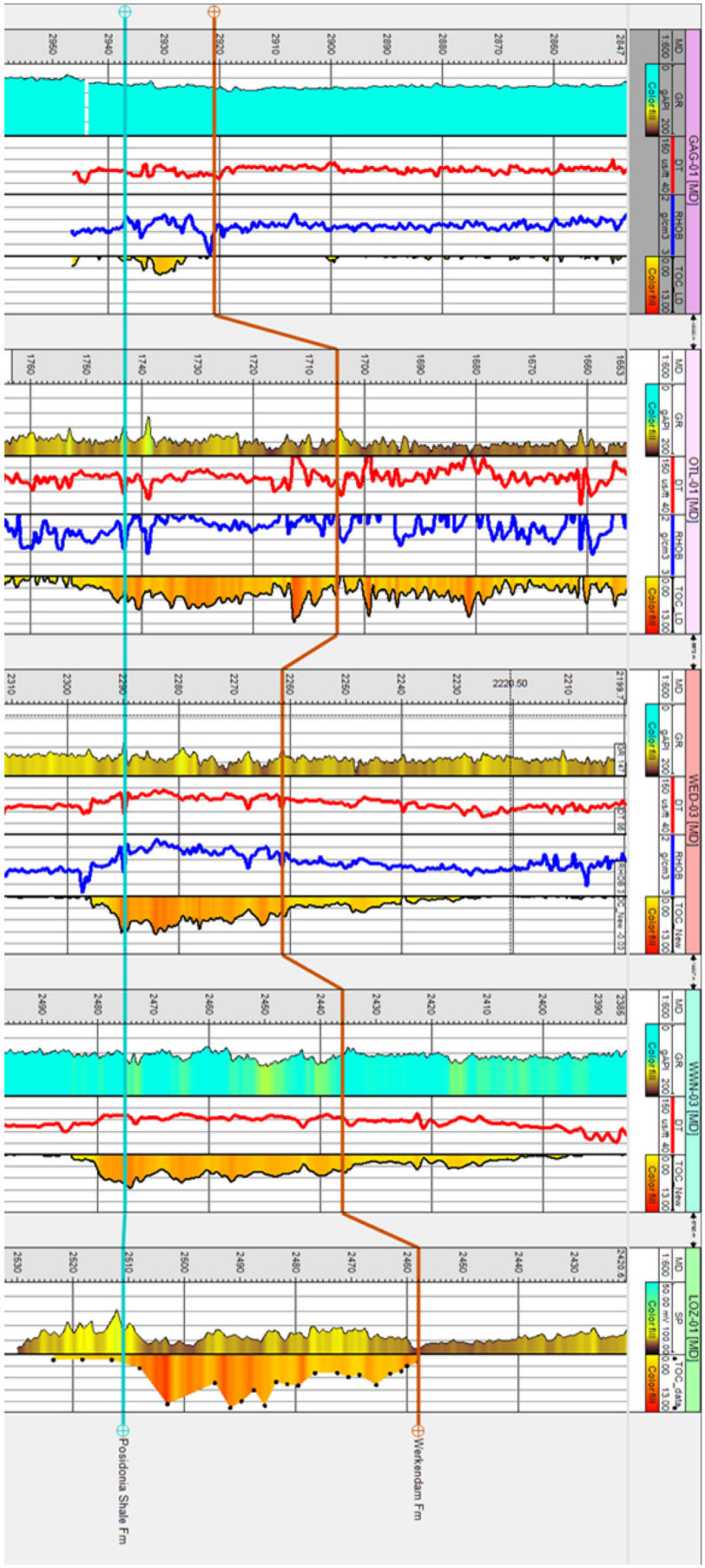

Fig. 3. Well log correlation for 5 wells in the onshore part of the West Netherlands Basin (see Fig. 1 for well locations). Gamma ray (GR), compressional sonic (DT), bulk density (RHOB) logs and log-derived *TOC* (TOC_{LD}) along measured depth (MD) are shown. The top (Werkendam Fm) and bottom (Posidonia Shale Fm) are indicated. Values for *TOC* from Rock Eval measurements on samples from well LOZ-01 are also indicated.

many cases, upfront assessment of shale prospectivity focusses on one of these three processes, or qualitatively combines different indicators (Jarvie et al., 2007; McKeon, 2011; Bust et al., 2013; Van Bergen et al., 2013). Comparison of different shale formations with different ranges of properties and identification of sweet spots in heterogeneous shales will benefit from methods that quantify the potential for hydrocarbon generation, storage and flow stimulation in a single parameter.

The main focus of this study is on using limited data in virgin shale basins to determine a single performance indicator that can be used to analyze shale prospectivity. The mean performance indicator is defined as the harmonic mean of three performance indicators that describe the potential for hydrocarbon generation, storage and flow stimulation. These key performance indicators are defined using different shale properties, including vitrinite reflectance, porosity, depth, thickness, sorbed gas content and brittleness. Different reservoir characterization techniques and modelling approaches are combined to quantify the shale properties. Because actual well production data are generally absent in virgin shale basins, shale properties are expressed relative to the properties of prospective North American shales in the performance indicators. The mean performance indicator can be mapped across parts of a virgin shale gas basin to identify the most promising targets. A contour map based on values of the mean performance indicator can be used to determine trends in potential shale productivity, locate sweet spots and point to preferred drilling sites in a virgin shale basin, thereby aiding shale exploration.

The Posidonia Shale Formation (PSF) in the Netherlands, mainly present in the West Netherlands basin and northern Dutch offshore sector, is used as a demonstration field case to illustrate the approach (Fig. 1). The formation is recognized as a source rock for conventional oil and gas occurrence across Europe (Lott et al., 2010), and is situated in a mature oil and gas basin in the Netherlands (Herber and De Jager, 2010). However, the Posidonia Shale Formation is relatively underexplored in the Netherlands as it has not yet been targeted for drilling in the Netherlands (Van Bergen et al., 2013; Zijp and Ter Heege, 2014). Due to its location in a mature oil and gas basin there is a considerable amount of data available such as of 2D and 3D seismic surveys, well logs, cores and core measurements (Fig. 2).

Several high resolution reservoir characterization studies have been performed using available data to obtain a detailed understanding of the vertical and lateral variation in depositional environment and heterogeneity in shale properties. Existing studies include basin modelling, well log interpretation, analysis of organic content and mineralogy, palynological correlations and –characterizations, seismic attribute analyses and stable isotope analyses, and outcrop studies that characterize the PSF from the small (nanometer) scale to the large (kilometer) scale (Fig. 2). Initial studies mainly focused on its role as source rock for conventional oil and gas in the Netherlands (see for example De Jager et al., 1996; Herber and De Jager, 2010, and references therein). Studies of Bouw and Lutgert (2012) and Van Bergen et al. (2013) focused on the PSF as a potential target for shale gas, and included new data from core measurements and well log interpretation. Both studies identified critical values for these parameters for the Posidonia Shale Formation (e.g. porosity, permeability, thermal maturity, thickness and depth, Table 1).

Van Bergen et al. (2013) also included maps of porosity and maturity (vitrinite reflectance) from basin modelling, and seismic attribute analysis of 3D seismic surveys showing structural complexity (i.e. fault blocks in horst-and-graben structures) for parts of the PSF located onshore in the West Netherlands Basin. These studies conclude that considerable amounts of gas are potentially present in the PSF, but low maturity and low brittleness ("soft shales") are challenges that may hamper economic hydrocarbon production. Verreussel et al. (2013) and Zijp et al. (2013) focused on integrating different reservoir characterization techniques to map out vertical and lateral variations in shale properties at high resolution as well as identifying prolific zones within the PSF. Godderij et al. (2014) and Ter Heege et al. (2014a, b) performed semi-analytical simulations of hydraulic fracturing and gas production yielding gas flow rates in the range of 5–30 MCM/day (0.2–1.0 MMCF/day) and cumulative gas production of 50–250 MMCM (1.8–8.8 BCF), assuming evenly spaced ("ideal") hydraulic fractures along a horizontal well of 1 km length and a well lifetime of 10 years. Recently, Zijp et al. (2015) provided additional detailed insight in vertical heterogeneity of the PSF in terms of shale thickness, composition, structure, depositional environment, and log response by studying outcrops of the Whitby Shale Formation in the Cleveland Basin of Yorkshire (United Kingdom), which can be regarded as an analogue for the PSF. None of these studies fully integrated the potential for hydrocarbon generation, storage capacity and flow stimulation. Moreover, mapping of sweet spots across the West Netherlands Basin has not been attempted.

The integrated approach for identifying sweet spots in underexplored shale gas basins using key performance indicators is demonstrated for part of the Posidonia Shale Formation in the West Netherlands Basin. It is shown how available data sources and different shale characterization approaches can be used to determine the performance indicators. Mapping of the mean performance indicators for the Posidonia Shale Formation shows clear trends in prospectivity across part of the West Netherlands Basin. A comparison between the Posidonia Shale Formation and prospective North American shales is performed to indicate the overall potential for gas production.

2. Geology and key properties of the Posidonia Shale Formation

2.1. Regional geology and spatial distribution

The Posidonia Shale Formation (PSF) is a grey to black shale of Toarcian age (182–180 Ma), found in a large part of the Southern Permian Basin reaching from the east coast of the United Kingdom in the West to central Germany in the East (Lott et al., 2010). In the United Kingdom, the formation is present as the Jet Rock Member (Yorkshire Basin, McArthur et al., 2008; Zijp et al., 2015), in France as Schistes Cartons (Paris and Aquitaine Basin), and in Germany as the Posidonienschiefer or Ölschiefer (Röhl et al., 2001; Frimmel et al., 2004). In the Netherlands, the formation is found at 1800–3800 m depth (Fig. 1). The thickness of the formation ranges from 15 to 30 m onshore to ~60 m in some offshore locations. At most locations the PSF is a bituminous dark-grey to brown-black fissile claystone (Fig. 2) deposited during a widespread oceanic anoxic event. The first anoxia, induced by a disturbance in the global carbon pool, is reflected by a pronounced shift in de $^{13}C/^{12}C$ ratio (or $\delta^{13}C_{org}$) of 7‰ towards more negative values (Röhl et al., 2001). This shift in the $\delta^{13}C_{org}$ is known as the Early Toarcian carbon isotope event (CIE). Several studies show that the duration of the Early Toarcian CIE is 930 Ka (McArthur et al., 2008), and that anoxia and black shale deposition lasted longer than the actual Early Toarcian CIE (Röhl et al., 2001). Furthermore pacing of the isotope trend is astronomically forced, suggesting that dissociating of gas hydrates are the likely source for the increase in light carbon (Hesselbo and

Table 1
Range of properties for the Posidonia Shale Formation and North American shales (see Table A.1 for explanation of symbols). Previous studies: B&L- Bouw and Lutgert (2012), VB-Van Bergen et al. (2013), US-Compilation from Wang and Gale (2009) and McKeon (2011). Note that North American shales may not be prospective for full range of properties. Values for this study are from wells in study area (c.f. Fig. 1, Table 2). Values in italic are (assumed) average values for the entire formation. *Gas saturation is assumed, or based on reported values for North American shales. Total and free gas content is calculated for assumed gas saturation.

Property [unit]	B&L	VB	This study	US
Depth [mTVD]		992–2937	1000–2928	1250–4270
Thickness [m]		14–61	16–53	15–150
Total organic carbon [wt%]	2–18	1–15	1.6–8.1	2–25
Porosity [%]	*17.2*	5–13	5–14	1–15
Permeability-GRI [10^{-12} D]	6–210			0.005–1200
Permeability-PD [10^{-6} D]	0.19–16			
Vitrinite reflectance [%]	<1.5–1.2	0.55–1.3	0.51–0.87	0.45–3.0
Brinell Hardness Number	*10*			18–80
Young's modulus [GPa]		1–50	8–25	7–70
Poisson's ratio [-]			0.33–0.39	0.13–0.27
Quartz content [wt%]	15–45		10–20	1–60
Carbonate content [wt%]	5–85		4–14	5–95
Clay content [wt%]	10–70 (*46*)		49–63	1–60
Brittleness index [%]			4.5–28.9	
Gas in mud [ppm]		244–175777		
Gas saturation (S_{gT}) [%]*	*50*	*23*		0.40–0.75
V_t/A [sm^3 CH_4/m^2 rock]*	676–844	260–460		
V_{tCH4}/V_r [sm^3 gas/m^3 rock]*	23–28	8–15		1–28
V_{fCH4}/V_r [sm^3 gas/m^3 rock]*	17–22	7–14		
V_{sCH4}/V_r [sm^3 gas/m^3 rock]*	*5.8*	*1*		

Pieńkowski, 2011; Suan et al., 2008). The probable cause for restricted circulation of sea water which led to the bottom anoxia was most like increased run-off of fresh water. This in turn is related to climate change. The high amounts of freshwater led to restriction in circulation in the then relatively shallow epiric sea (McArthur et al., 2008; Frimmel et al., 2004). Recently it was concluded that the depositional environment is temporarily and spatially more variable with changing oxic and anoxic conditions and high energy events (Trabucho et al., 2012; Van Bergen et al., 2013; Verreussel et al., 2013).

The PSF is proven to be a source rock for oil and gas in the Netherlands as well as Germany (Van Balen et al., 2000; De Jager and Geluk, 2007; Lott et al., 2010). Most of the Dutch onshore oilfields are believed to be sourced from the PSF. The PSF may have acted as a source rock together with the surrounding Jurassic Aalburg and Sleen Formations (De Jager et al., 1996; Bouw and Lutgert, 2012).

2.2. Key properties using shale characterization approaches

Available data for the Dutch PSF includes (vintage) well logs from around 70 wells and core material from 5 wells. Available data sources are limited by the fact that data collection was not specifically targeted at the PSF, but (vintage) data is available because of exploration to deeper (Triassic Buntsandstein) tight sandstone reservoirs. Accordingly, estimating shale gas properties based on these data is prone to uncertainties, and, can only be used to give best estimates of shale properties. More detailed analysis may be performed if data collection is specifically targeted at shale exploration and properties can be evaluated by cross-comparing well logs or properties from different data sources (as is the case for most prospective North American shales, see for example Sondergeld et al., 2010; Bust et al., 2013). In this study, well log interpretation, core analysis and basin modelling is combined to determine key shale properties (Table 2).

Table 2
Shale properties of the Posidonia Shale Formation at different well locations in the onshore part of the West Netherlands Basin (c.f. Fig. 1). Note that *TOC* for wells GAG-01 and LOZ-01 are from measurements on core material.

Property	Z	Δz	TOC	R_o	ϕ_{tot}	E_{dyn}	ν_{dyn}	BI_{dyn}	BI_{min}
Unit	m	m	wt%	%	%	GPa	–	–	–
Well									
GAG-01	2912	16	1.6	0.87	5	25	0.33	28.9	22.9
KWK-01	1693	28	5.9	0.58	10	9	0.39	5.5	–
LOZ-01	2458	53	6.5	0.77	10	–	–	–	17.2
MRK-01	1283	29	7.5	0.57	11	16	0.36	16.3	–
OTL-01	1541	33	4.9	0.58	14	10	0.38	7.7	–
WAA-01	1613	28	6.1	0.51	12	8	0.39	4.5	–
WED-02	2197	23	5.5	0.78	-	10	0.39	7.1	–
WED-03	2192	24	5.5	0.78	11	9	0.39	5.8	14.0
WLK-01	1000	24	8.1	0.54	9	8	0.39	4.8	–
WWN-03	2096	27	4.6	0.79	12	10	0.39	7.7	–
Average	1899	28	5.6	0.68	10	12	0.38	9.8	18.0
Minimum	1000	16	1.6	0.51	5	8	0.33	4.5	14.0
Maximum	2912	53	8.1	0.87	14	25	0.39	28.9	22.9

2.2.1. Well log interpretation

Available well logs were used to correlate the PSF wells (Fig. 3). A detailed zonation of the shale formation was made using gamma ray, sonic, density, and deep resistivity logs, where available (Verreussel et al., 2013; Zijp et al., 2015). The different zones and their respective log characteristics were correlated to biofacies, mineralogy, and organic geochemistry to reveal changes in depositional setting and –conditions. Well log correlation supported seismic interpretation aimed at mapping out the PSF depth distribution in the Netherlands basin (Fig. 1), and provided local data on the thickness (Table 2).

Total organic carbon (TOC_{LD}) content was determined using the gamma ray, sonic, and deep resistivity logs (Passey et al., 1990). This method correlates TOC_{LD} to curve separation ($\Delta logR$) of deep resistivity and sonic logs

$$TOC_{LD} = 10^{(2.297-0.1688LOM)}\Delta\log R \quad (1)$$

$$\Delta logR = \log_{10}\frac{RESD}{RESD_{BASE}} + 0.02(DT - DT_{BASE}) \quad (2)$$

with TOC_{LD} in wt% (assuming that curve separation is a quantitative proxy for *TOC*). *LOM* indicates the level of organic metamorphism (Hood et al., 1975), which can be related to vitrinite reflectance (*Ro*, Passey et al., 2010).

Deep resistivity (*RESD*) and sonic travel time (*DT*) curves need to be scaled so that resistivity and sonic travel time baselines ($RESD_{BASE}$ and DT_{BASE}) overlap in log intervals where water-saturated, organic-poor shales are present. If properly scaled, *ΔlogR* can be measured in log intervals where organic-rich shales are present. The accuracy of the method critically depends on (1) accurate baselines determined by the presence of non-source organic-poor shales of similar age in the stratigraphic interval or by the accuracy of different baselines for zones within the shale with varying mineralogy or pore water salinity, (2) *LOM* determination (generally determined by accuracy and availability of a *LOM*-R_o relation), (3) availability of local calibration to *TOC* measurements on shale core samples, and (4) variations in the abundancy of pyrite between different shale intervals that strongly shale resistivity (Passey et al., 2010; Sondergeld et al., 2010; Bust et al., 2013; Crain and Holgate, 2014). In practice, absence of organic-poor shale intervals will result in underestimation of *TOC* as baselines will be set at intervals that contain significant levels of *TOC*. Direct determination of *LOM* is rare (Crain and Holgate, 2014), so analysis of R_o or local calibration of *ΔlogR-TOC* relations will are required for accurate results. The presence of pyrite results in underestimation of *TOC* (Sondergeld et al., 2010). If applied to the PSF, the method yields excellent correlation between TOC_{LD} and *TOC* from measurements on core samples for well LOZ-01 (*LOM* = 9, Fig. 3). The analysis yields TOC values between 1.6 and 8.1 wt% (Table 2, see also Bouw and Lutgert, 2012; Van Bergen et al., 2013; Ter Heege et al., 2014a for application to the PSF).

Total porosity (ϕ_{tot}) was determined by the volume average of densities of the bulk shale (ρ_{bulk}), solid constituents (ρ_{solid}), non-hydrocarbon pore fluid (ρ_f) and hydrocarbons (ρ_{hc})

$$\rho_{bulk} = \phi_{tot}S_{wT}\rho_f + \phi_{tot}(1 - S_{wT})\rho_{hc} + (1 - \phi_{tot})\rho_{solid} \quad (3)$$

with S_{wT} the water saturation relative to total porosity (i.e. hydrocarbon –filled porosity is given by $\phi_{hc} = (1 - S_{wt})\phi_{tot}$). The density of solid constituents was determined by the weight average of densities of the shale matrix (ρ_{mat}) and organic matter (ρ_{TOC})

$$\rho_{solid} = TOC\rho_{TOC} + (1 - TOC)\rho_{mat} \quad (4)$$

Eqs. (3) and (4) can be written in terms of total porosity

$$\phi_{tot} = \frac{\rho_{bulk} - \rho_{mat} + TOC\rho_{mat} - \rho_{TOC}TOC}{TOC\rho_{mat} - \rho_{mat} - \rho_{TOC}TOC + S_{wT}\rho_f + (1 - S_{wT})\rho_{hc}} \quad (5)$$

This expression for ϕ_{tot} has the advantage that all terms can be determined from well logs, core analysis or measurements from North American shales. ρ_{bulk} can be determined using the *RHOB* log, *TOC* can be determined using the TOC_{LD} curve, ρ_{mat} can be determined using a mineral model for the shale (based on well logs or core analysis), and ρ_f, ρ_h, ρ_{TOC} and S_{wT} should be estimated from analogue (North American) shales (as resistivity or NMR logs are generally unavailable for the PSF, c.f. Van Bergen et al., 2013). It is assumed that the density of hydrocarbons and pore fluid in the shale matrix is the same as in the organic matter, and there is no explicit distinction between porosity, free- and adsorbed hydrocarbons, or water saturation in the shale matrix and organic matter. It should be noted that in Eq. (5) volume average densities are used to distinguish between solids and pores (c.f. Eq. (3)), while weight average densities are used to distinguish between organic matter and shale matrix (c.f. Eq. (5)). Alternative expressions for ϕ_{tot} exist with different assumptions regarding the contribution of *TOC* to bulk density or distinction between porosity in the shale matrix and in the organic matter (Sondergeld et al., 2010; Bouw and Lutgert, 2012; Bust et al., 2013). The analysis yields ϕ_{tot} values between 5 and 14% (Table 2, note that ϕ_{tot} for well LOZ-01 are from measurements on core material).

For wells with available sonic logs, elastic properties of the shale, described by the dynamic Young's modulus (E_{dyn}) and Poisson's ratio (ν_{dyn}), were derived. For wells with a dipole sonic log, E_{dyn} and ν_{dyn} were calculated from compressional (v_p) and shear (v_s) sonic wave velocities (Fjaer et al., 2008)

$$E_{dyn} = \rho_b v_s^2 \frac{3v_p^2 - 4v_s^2}{v_p^2 - v_s^2} \quad (6)$$

$$\nu_{dyn} = \frac{\left(v_p^2 - 2v_s^2\right)}{2\left(v_p^2 - v_s^2\right)} \quad (7)$$

with v_p and v_s in km/s. If only a monopole sonic log is available, v_s was calculated from v_p using an empirical relation form mudstones (Castanga et al., 1985)

$$v_s = \frac{v_p - 1.16}{1.36} \quad (8)$$

The analysis yields dynamic elastic moduli, while static moduli are most relevant in determining the efficiency of hydraulic fracturing in terms of flow stimulation (Economides and Nolte, 2000; Fjaer et al., 2008). Dynamic elastic moduli can be related to static mechanical properties using laboratory measurements (Eissa and Kazi, 1988; Sone and Zoback, 2013). Empirical relations between static and dynamic elastic moduli critically depend on many factors, including mechanical anisotropy as well as local stress state (Sone and Zoback, 2013). Therefore, application of such relations to convert sonic log derived dynamic moduli to static moduli for different shales is not straightforward (Fjaer et al., 2008). Static elastic moduli are generally observed to consistently increase with dynamic moduli for prospective shales (King, 2010), and the brittleness of shales is generally observed to increase with increasing dynamic Young's modulus and decreasing dynamic Poisson's Ratio (Rickman et al., 2008; Yang et al., 2013). Therefore, an empirical brittleness index can be defined based on the relative magnitude of dynamic elastic moduli normalized to the range of elastic moduli for shales (Rickman et al., 2008)

$$BI_{dyn} = \frac{1}{2}\left(\frac{E_{dyn} - E_{dyn}^{min}}{E_{dyn}^{max} - E_{dyn}^{min}} + \frac{\nu_{dyn}^{max} - \nu_{dyn}}{\nu_{dyn}^{max} - \nu_{dyn}^{min}}\right) \quad (9)$$

The analysis yields values for E_{dyn} of 8–25 GPa, ν_{dyn} of 0.33–0.39 and BI_{dyn} of 4.5–28.9% (Table 2).

2.2.2. Core analysis

Available shale samples from different wells (e.g., GAG-01 and LOZ-01) were used for total organic carbon (*TOC*) measurements as well as Rock-Eval measurements that are indicative of the hydrocarbon generation potential of the shale formation (Table 2). *TOC* measurements were compared to log-derived values (TOC_{LD}, c.f. Eq. (1), Fig. 3), which were used to correlate *TOC* laterally, over large parts of shale formation. Light microscopy on thin sections and FIB-

SEM were used to identify variations in mineralogical compositions, grain size, and microstructure of shale matrix, laminations and fractures infill (Fig. 2). Shale samples were also used to characterize natural fractures at the centimeter scale, in particular fracture fill, orientation, and density. The mineralogy of the shale samples was also used to calculate a brittleness index (Jarvie et al., 2007)

$$BI_{min} = \frac{Qz}{Qz + Ca + Cl} \tag{10}$$

This index was used together with the brittleness index based on dynamic elastic moduli (c.f. Eq. (9)) to indicate shale brittleness. It should be noted that the use of shale brittleness based on mineralogy or dynamic elastic moduli to indicate the efficiency of flow stimulation is poorly defined, and trends based on different brittleness indices may not be consistent (Yang et al., 2013). The analysis yields values for BI_{min} of 16–23% (Table 2).

2.2.3. Basin modelling

Basin modelling was used to determine maturity and porosity across the PSF (Fig. 4). The maturity and porosity map of the study area is part of a larger model of the West Netherlands Basin and Roer Valley Graben. About 70% of the Dutch onshore and offshore areas has been included in the basin models underpinning the maps. A detailed description of the modelling process and the assumptions behind the model are given in Nelskamp and Verweij (2012) and Van Bergen et al. (2013).

The present-day static depth model of the subsurface is used for temperature and pressure forward modelling. The depth model and forward models are based on the present-day geological interpretation of the subsurface (depth, age and lithology of the formations) and an interpretation of the thermal history (past sediment surface temperatures and basal heat flow). Compared to maps published by Van Bergen et al. (2013), updated basin models and latest geological interpretation of the subsurface is used to construct maturity and porosity maps shown in Fig. 4. The geological evolution of the study area through time is modelled and calibrated against thermal indicators and rock measurements (present-day formation temperatures, vitrinite reflectance or other maturity indicators, porosity and pressure measurements). Depending on the structural complexity of the area and degree of exploration, the resulting models are subject to different levels of uncertainty. The Netherlands are very mature in terms of conventional oil and gas exploration with a large number of deep exploration and production wells and large areas with 3D seismic coverage. However, due to significant uplift and erosion during the Jurassic and Cretaceous, parts of the stratigraphic section are eroded, increasing the uncertainty of the models. The maturity map is calibrated to vitrinite reflectance measurements from organic rich rocks and corrected for present-day formation temperatures. The porosity map is calibrated to two porosity measurements for the PSF, and the applied mechanical compaction model for mudstones was adjusted using porosity measurements from the Dutch subsurface (Nelskamp and Verweij, 2012). The resolution of the maps is 1 km × 1 km, which means existing smaller scale structural elements might not be visible due to limited resolution. The maturity in the study area is relatively low (<1%Ro) with locally maturities up to ~1.1. Previous studies on the organic matter of the PSF from Germany indicate that this maturity relates to the oil-to- early gas window (Bernard et al., 2012). Oil maturity is also supported by the presence of oil fields that have been sourced from the Posidonia Shale Formation in the area (Herber and de Jager 2007, Lott et al., 2010).

3. Geology, key properties and hydrocarbon production of North American shales

More than 70 shale plays have been identified in North America (Wang and Gale, 2009). The comparison between North American and Dutch shales in this study focusses on four plays with shale as the source rock, i.e. the Marcellus Shale Formation, the Bakken Formation, the Haynesville Shale Formation, and the Barnett Shale Formation. Key properties of the shales and production data were assessed on the basis of data in the public domain (Table 3, Fig. 5). Similar properties were analyzed as for the Posidonia Shale Formation, including depth and thickness of the reservoir, total organic content, porosity, permeability, thermal maturity and brittleness index (c.f. Table 2). Where possible, shale properties were determined on a regional scale to assess ranges in properties for the entire shale and on a local scale to link specific properties to areas or wells with high productivity. The wells were selected based on their location and availability of data (Table 3). The following review of the geology, key properties and hydrocarbon production of North American gas shales is brief and by no means comprehensive (i.e. all data are taken at face value). More comprehensive reviews can be found in the vast amount of literature published on these shales (see for example the studies listed below and references therein). Compilations of data for different shales are from publications of the Energy Information Agency (EIA, 2011, 2015a,b), United States Geological Survey (USGS, e.g., Charpentier and Cook, 2010, 2013), United States Department of Energy (DoE), Department of Environmental Protection, Pennsylvania (DEPP), McKeon (2011) and Ramurthy et al. (2011). Resource estimates and drilling productivity from EIA (2011, 2015a,b) are used so that methodologies used to derive the estimates are consistent and can be used to identify rough trends with regional shale properties.

3.1. Marcellus Shale Formation

The Devonian Marcellus Shale Formation (MSF) covers an area of roughly 140.000 km^2 in the Appalachian Basin, extending southward from central Pennsylvania and southwestern New York into eastern Ohio and West Virginia (Fig. 5a). Specific data on reservoir properties and gas production from the MSF (Table 3) is taken from Wrightstone (2009), Carter et al. (2011), Lee et al. (2011), Gargouri (2012). The MSF is deposited in an anoxic deep water environment with sedimentation controlled by the Acadian orogeny. On a regional scale, depth is below 1500 m and average thickness is 30 m. Depth and thickness of the formation increase towards the east with a thickness reaching 75 m in northeastern Pennsylvania. The MSF is one of the main shale gas resources in the northeastern United States. Estimated GIP is in the range of 295–2700 TCF (8350–76450 BCM), of which ~10% is estimated to be recoverable. In June 2015, daily gas production from the MSF was 16737 MMCF/day (0.47 BCM/day, month over month). In 2011, cumulative gas production was 822 BCF with an average production of 1.3 MMCF/day. Gas production is not uniform across the state with the most productive areas in the middle and northeastern parts of the basin (i.e. Bradford, Susquehanna, Wyoming counties, Fig. 5a). Local data is analyzed for the King 2 well in Susquehanna county, the Johnston 1-1H well in Wyoming county and the Minard Run Exploration No.1 well (PA1 EGSP) in McKean county (Table 3, Fig. 5a).

3.2. Bakken Formation

This summary for the Upper Devonian-Lower Mississippian Bakken Formation (BF) focusses on the area located in the Williston Basin, North Dakota (Fig. 5b). Specific data on reservoir properties

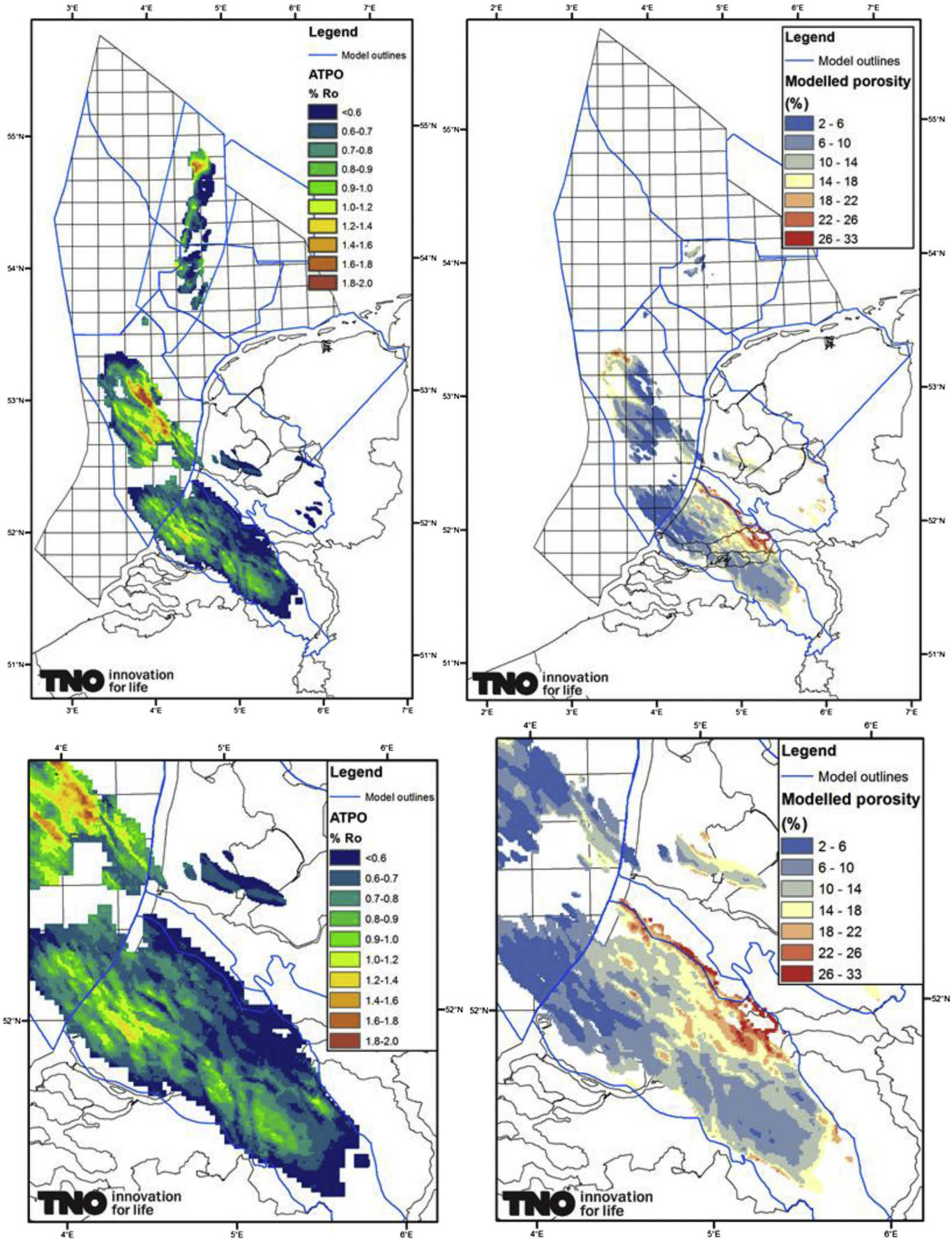

Fig. 4. Maturity and porosity maps for the Posidonia Shale Formation determined using basin modelling.

and hydrocarbon production are taken from Webster (1984), Pitman et al. (2001), Sorensen and Terneus (2008), Jarvie et al. (2011), and from the North Dakota Geological Survey. The BF consist of upper and lower black, organic rich shales separated by a calcareous fine grained sand and silt stone (middle) member that is the main oil reservoir. The organic rich shales act both as source rock and seals. Accordingly, reservoir properties cannot be directly compared to the other shales but analysis of the maturity of neighbouring shales is of interest. In North Dakota, the Bakken Formation is located at an average depth of 2800 m. In June 2015, daily oil and gas production from the BF was 1267 MBBL/day and 1499 MMCF/day (0.042 BCM/day, month over month), respectively. In 2013, the BF produced 305 BCF (8.6 BCM) of gas and 285 million barrels of oil. Counties with highest production include McKenzie, Mountrail, Williams and Dunn (Fig. 5b). Local data is analyzed for the Parshall Area, including the ND 1–05H well in the Parshall Field and the Braaflat 11-11H well in the Sanish Field (Mountrail County, Table 3). The Parshall Field and its extensions are considered to be the largest oil field in size in North America (c.f. Fig. 5b).

3.3. Haynesville Shale Formation

The Late Jurassic Haynesville Shale Formation (HSF) covers an area of roughly 25,000 km^2 across East Texas and Northwest Louisiana (Fig. 5c). This review focusses on the occurrence of the HSF in North Louisiana. Data on reservoir properties and hydrocarbon production (Table 3) are taken from Milici and Swezey (2006), Parker et al. (2009), Sone et al. (2010), Hammes et al. (2011), Kaiser and Yu (2011), Hammes and Frébourg (2012), Nunn (2012), Kaiser and Yu (2013). The HSF is underlain by the Smackover Limestone and overlain by the Bossier Shale and Cotton Sandstone formations. It is considered to have favourable properties due to high overpressures, which promote porosity, gas content and brittleness. Because the pore pressure is near the fracture pressure, it is naturally fractured in some areas and relatively easy to fracture. In North Louisiana, the HSF is located at depths ranging from 3100 to 4200 m and the thickness ranges from 30 m in the northwestern part of the play to about 120 m in the southeastern part. In June 2015, daily oil and gas production from the HSF was 58 MBBL/day

Table 3
Shale properties and hydrocarbon production on regional (formation) and local scale (field or well) for the Marcellus Shale Formation, Bakken Formation, Haynesville Shale Formation and Barnett Shale Formation (see text for data sources). Quoted values are average values or ranges of values, unless otherwise indicated. If not specified, regional brittleness values are calculated from average mineralogical composition (based on the compilation by McKeon, 2011). Properties of the Bakken Middle Member tight sandstone are not included in the minimum and maximum values. *GIP* and *OIP* are estimates of gas in place and oil in place from EIA (2011). Regional Q_{cum} values indicate average estimated ultimate recovery (EUR, EIA, 2011 and Charpentier and Cook, 2013), local Q_{cum} values are cumulative production per well from in the local area around the well (over different periods, c.f. Figs. 5 and 30 year production projection for Barnett). Regional Q_{well} values indicate new-well gas production per rig (EIA, 2015a,b), local Q_{well} are quoted in literature.

Property	Z	Δz	TOC	R_o	ϕ	κ	Mineralogy	BI_{min}	GIP OIP	Q_{cum}	Q_{well} (year)
Unit	m	m	wt%	%	%	mD	Qz; Ca; Cl wt%	–	TCF 10^9 BBL	BCF MBBL	MMCF/d MBBL/d
Shale play											
MARCELLUS											
Regional	*1400–2600*	*15–90*	*2–10*	*0.8–3.0*	*0.5–8.0*	*0.00001–0.1*	*10–40; 5–20;25–60*	*0.1–0.6*	*gas:410*	*1.18*	*8.2 (2015)*
King 2		65		2.75						2.0–3.8	16.4
Johnston 1 1H		73		3.0						2.0–3.8	
PA1 EGSP	1550	25	2.46	1.26						1.0–2.0	
BAKKEN											
Regional (shales)	*2400–3350*	*2–44*	*5–21*	*0.3–0.6*	*2–12*	*0.01–0.5*	*15–70;15–65; 3–20*	*0.2–0.8*			
Upper Shale	>2400	2–5	5–21			0.01–0.5					
Lower Shale	<3350	24–44	8–21			0.01–0.5					
Middle Member		20			1.0–16.0	0.0001–7.0			*gas: - oil: 3.59*	*- 550*	*0.6 (2015) 0.6 (2015)*
ND 1–05H (Parshall Field)	2868	22	0.5–20	0.3–0.6	5.0–7.0	<1				– 300	
Upper Shale	2868	5	12	0.6	7.0						
Lower Shale	2885	5	15	0.6	7.0						
Middle Member	2873	12	0.5	0.3	5.2	0.01	30; ?; 15				
Braaflat 11–11H (Sanish Field)	3007	33	0.5–15	0.3–0.6	6.4					– 150–300	
Upper Shale	3007	3	8	0.6							
Lower Shale	3026	14	8	0.6							
Middle Member	3010	16	0.5	0.3			35; ?; 15				
HAYNESVILLE											
Regional	*3100–4200*	*18–120*	*1–5.5*	*1–1.43*	*8.0–15.0*	*0.000005–0.001*	*25–52;13–44; 12–20*	*0.3–0.7*	*gas: 75 oil: -*	*3.57 -*	*6.0 (2015) 0.03(2015)*
BARNETT											
Regional	*1645–2895*	*30–150*	*2.6–11.5*	*0.48–2.64*	*1.5–6.0*	*0.00005–0.02*	*40–60; 5–30; 6–30*	*0.4–0.8*	*gas: 43*	*1.42*	*hor.: 1.7 vert.: 0.7 (peak,2003)*
2 T P. Sims vert. well, Wise County				1.65						2.025	1.0–2.0
noncore vertical wells				0.8–0.9						0.5–2.0	0.1–0.5
horizontal wells				1.0						<2.8	>1
Erath County											
MINIMUM	**1400**	**3**	**0.5**	**0.3**	**0.5**	**0.000005**		**0.1**			
MAXIMUM	**4200**	**150**	**21**	**3.0**	**16**	**0.1**		**0.8**			

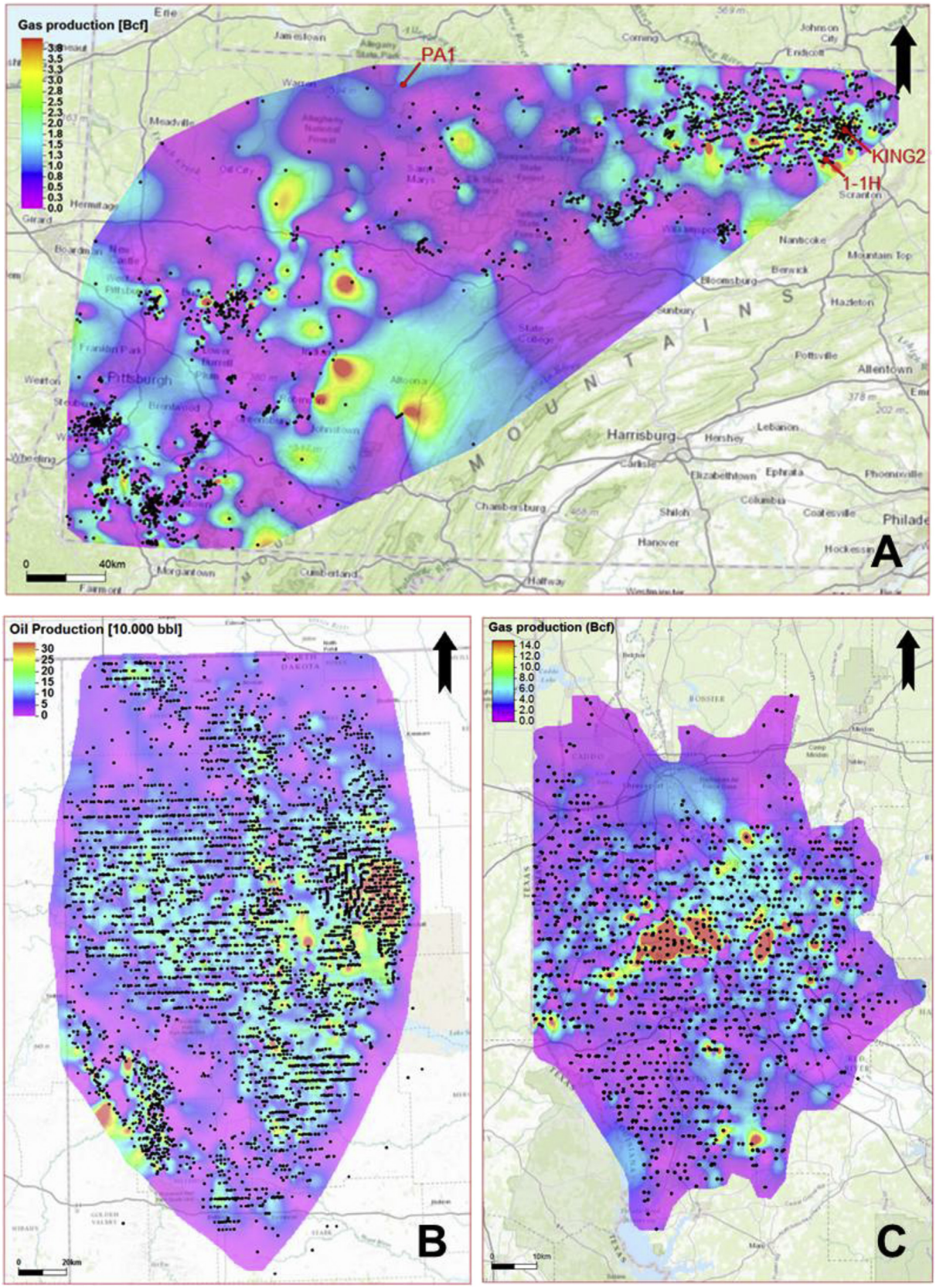

Fig. 5. Cumulative hydrocarbon production from the (A) Marcellus Shale Formation (over period 2000–2013, data from the Department of Environmental Protection, Pennsylvania) with locations of wells (c.f. Table 3), (B) Bakken Formation (over period 1961–2012, data from the Oil and Gas Division of the North Dakota Industrial Commission) and (C) Haynesville Shale Formation (over period 2007–2013, data from the Louisiana Department of Natural Resources).

and 7034 MMCF/day (0.20 BCM/day, month over month), respectively. Total cumulative production is estimated to be 5774 BCF (184 BCM, over the period 2007–2012, Kaiser and Yu, 2013). Cumulative gas production per well may be as high as 7.5 BCF (0.21 BCM) with production rates as much as 3.0 MMCF/day (85 MCM/day). The most productive areas are currently the De Soto and the Red River Parishes areas that produced up to 14.0 BCF (0.40 BCM) of unconventional gas (Fig. 5c).

3.4. Barnett Shale Formation

The Barnett Shale Formation (BSF) is located in the Fort Worth Basin (Texas, USA). Specific data on reservoir properties and production (Table 3) is taken from Montgomery et al. (2005), Bowker (2007) and Jarvie et al. (2007). The BSF consists of five lithostratigraphic zones (1) black shale, (2) lime grainstone, (3) calcareous black shale, (4) dolomitic black shale, and (5) phosphatic black shale. It is a relatively thick unit with a reservoir thickness in the range of 15–305 m (average thickness of 107 m). Maturity is highest in the northwestern part of the Fort Worth Basin (Wise, Denton and Tarrant counties). Outcrops of immature shales with average TOC of 11.5wt% are present in the South (Lampasas and Williamson counties). Maximum production is from the zone within the formation with a mineralogy that consist of 45% quartz and 27% clay (BI_{min} approximately 0.6). Daily gas production from the BSF is expected to peak around 5.6 BCF/day (0.16 BCM/day) in 2015 (Browning et al., 2013). In 2003, the cumulative gas production of Barnett wells was about 0.8 TCF (23 BCM). Local production data for vertical and horizontal wells in areas of different maturity from the study of Jarvie et al. (2007) is included.

4. The use of shale properties as key performance indicators for hydrocarbon production

Synthesis of the data from North American shales to obtain a direct relation between shale properties and hydrocarbon production is not straightforward because (1) hydrocarbon production is controlled by the complex interplay of several properties and site-specific geological evolution and setting, and (2) limited production data for local wells is available in the open literature which hampers a systematic analysis of variation in production with shale properties. However, the data inventory can be used to determine ranges in properties of prospective shales (Table 3). The current approach is to determine the potential for hydrocarbon production by considering that production from shales is controlled by (1) hydrocarbon generation, (2) hydrocarbon storage capacity, and (3) efficiency of flow stimulation. The inventory is used to determine specific properties for prospective North American shales indicating the potential for hydrocarbon generation, storage and flow stimulation that can be directly compared to properties of the Posidonia Shale Formation. The potential for hydrocarbon production is quantified using key performance indicators that are based on the magnitude of local PSF properties relative to ranges of prospective shale properties.

4.1. Relation between shale properties and hydrocarbon production

The potential for hydrocarbon generation can be analyzed on the basis of organic matter (*TOC*) and vitrinite reflectance (R_o). Organic matter is the source for hydrocarbons, while vitrinite reflectance is a measure of thermal hydrocarbon maturity (Jarvie et al., 2007; Hartwig and Schulz, 2010; Van Bergen et al., 2013). Upon maturation, part of the original *TOC* is converted into hydrocarbons while another part is retained as hydrogen-poor *TOC*. As R_o increases upon maturation, there is an approximate inverse relation between *TOC* and R_o for present-day *TOC* between ~1 wt% and ~8 wt% (Fig. 6).

Considering that part of the original *TOC* is retained as hydrogen-poor *TOC*, shales with present-day *TOC* < 1 wt% have had limited available source for hydrocarbon generation. The North American shales with present-day *TOC* > 8 wt% either are immature (as is illustrated for the BSF) or have generated oil (as illustrated for the BF). Based on the compilation and production data for the BSF, a division of R_o in terms of oil and gas generation gives a rough indication of average gas production per well (Fig. 6). The Middle Member of the BF does not follow these trends because it is not a shale source rock but a calcareous fine grained sand and siltstone (sst) reservoir that contains oil generated from the over- and underlying shale formations. *TOC* values for the PSF are determined from both core measurements and well logs (c.f. Table 2), and R_o values at the well locations are from basin modelling calibrated by Rock Eval measurements (c.f. Fig. 6). *TOC* values for the PSF plot in the range of *TOC* of North American shales that have generated gas. R_o values plot at the lower bounds for these shales and in the oil generation window for BSF.

For the analysis of hydrocarbon storage potential both the storage of free and sorbed need to be considered (Fig. 7). Free hydrocarbons resides in available pore space, while sorbed hydrocarbons are chemically adsorbed or physically absorbed to the shale matrix (Jarvie et al., 2007).

The storage capacity of free hydrocarbons (SC_f) is analyzed on the basis of shale thickness (Δz), porosity (ϕ) and depth (Z), and can be expressed as

$$SC_f = \Delta z \phi_{hc} F_{expZ} \tag{11}$$

with SC_f in standard volume of hydrocarbons per unit area (in sm^3/m^2), ϕ_{hc} denoting the open porosity available for storage of hydrocarbons and F_{expZ} denoting a depth-dependent expansion factor (in sm^3/m^3) that adjusts hydrocarbon volume in the reservoir to standard volume at the surface ($F_{expZ} = 1/B_g$ for gas and $F_{expZ} = 1/B_{oi}$ for oil, EIA, 2011). In this study, storage capacity is analyzed for gas. F_{expZ} for gas is calculated as the ratio between the density of methane at depth of the shale and the density of methane at the surface using equations of state for methane (Lemmond et al., 2011). Methane density at depth of the shale is determined for hydrostatic pressure ("lower bound") and 30% overpressure ("upper bound"), using consistent temperature and pressure gradients to eliminate effects of local differences in reservoir conditions (i.e. only effects of different shale properties are taken into account). In resource estimates hydrocarbon-filled porosity (ϕ_{hc}) and total porosity (ϕ_{tot}) are usually related by hydrocarbon saturation (S_{hc}, i.e. $S_{hc} = S_{gT}$ for gas saturation $S_{hc} = S_{oT}$ for oil saturation of pore space, EIA 2013). For underexplored shales like the PSF, data on saturation is often subject to large uncertainty (estimates for the PSF range from 0.23 to 0.50, Bouw and Lutgert, 2012; Van Bergen et al., 2013, c.f. Table 1). As the current analysis aims to identify trends in hydrocarbon production instead of resource estimates and to avoid the use of uncertain S_{hc} values, upper bounds for SC_f are calculated by taking ϕ_{hc} equal to total porosity (ϕ_{tot}) in Eq. (11). Accordingly, the quoted SC_f should be regarded as an upper bound (SC_f^{max}). The storage capacity of sorbed hydrocarbons (SC_s, in standard volume of hydrocarbons per unit area, sm^3/m^2) is analyzed on the basis of shale thickness, organic content and depth. SC_s can be calculated by multiplying shale thickness with the volume of sorbed hydrocarbons per volume of shale (V_s). For methane, the dependence of sorbed methane V_{sCH4} on pressure (P) can be described using Langmuir isotherms (Langmuir, 1918; Gasparik et al., 2012; Heller

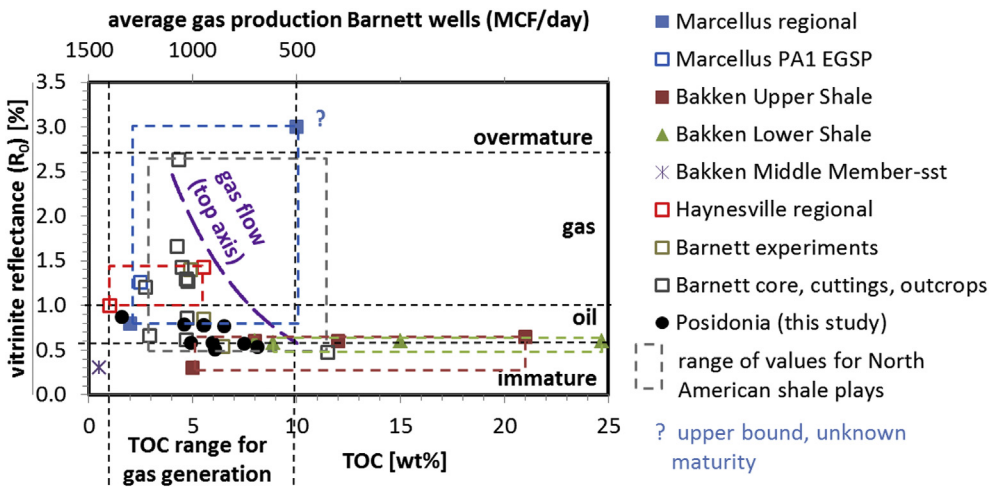

Fig. 6. Maturities of the Marcellus Shale Formation, Bakken Formation, Haynesville Shale Formation, Barnett Shale Formation in North America and the Posidonia Shale Formation in the Netherlands. Ranges of vitrinite reflectance (R_o) data from Rock-Eval measurements on core material and basin modelling (Posidonia) are plotted again total organic carbon content (*TOC*) from Rock-Eval measurements on core material and well log interpretation (c.f. Eqs. (1) and (2)). Maturity windows for different R_o values and average gas flow from wells (purple dash line) are based on analysis for the Barnett Shale Formation (Jarvie et al., 2007).

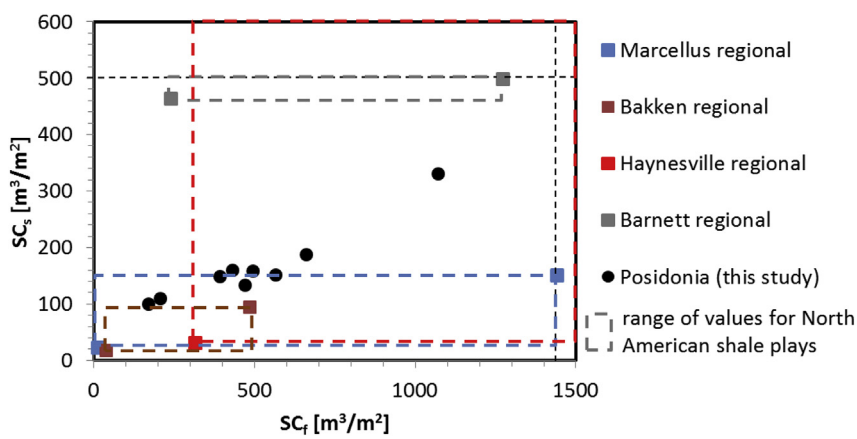

Fig. 7. Storage capacity (volume of methane per unit area of shale) for free gas (SC_f) and sorbed gas (SC_s) of the Marcellus Shale Formation, Bakken Formation, Haynesville Shale Formation, Barnett Shale Formation in North America and the Posidonia Shale Formation in the Netherlands.

and Zoback, 2014). A general expression for methane SC_s at depth is given by

$$SC_s = \Delta z V^Z_{sCH4} \tag{12}$$

with SC_s in standard volume of methane per unit area (in sm^3/m^2), and P and T required for the Langmuir isotherm determined by Z and the local thermal and pressure gradients. Methane adsorption in shales is dependent on many properties, including *TOC* and clay mineralogy. Methane adsorption isotherms are shale-specific and not available for all shales or all relevant *P-T* conditions. Extrapolation of values to account for variation in shale properties or subsurface conditions is ambiguous. Therefore, values for V^Z_{sCH4} are determined using experimental data of pressure-dependent methane adsorption for the different shales at face value without correcting for differences in, for example, *TOC* or temperature. Experimental data at relevant pressures for the MSF, BSF and PSF are used for upper and lower bounds of V^Z_{sCH4} (Gasparik et al., 2012; Heller and Zoback, 2014). The upper bound for HSF SC_f and SC_s is excluded as it is a clear outlier compared to the other North American shales. SC_f and SC_s values for the PSF are in the same range of values as for the North American shales (roughly between values for the BF and BSF).

The potential for efficient flow stimulation can be determined using the brittleness index based on mineralogy (BI_{min}, c.f. Eq. (10)) or brittleness index based on ranges of dynamic elastic moduli (BI_{dyn}, c.f. Eq. (9), Figs. 7, 8). In addition, the brinell hardness number (*BHN*) can be analyzed which is a proxy for proppant embedment, i.e. the potential for proppant embedment is high in shales with low *BHN*. Efficiency of flow stimulation is low in shales with low *BHN* for frac fluids with low proppant concentrations (Ramurthy et al., 2011). Accordingly, tailored frac designs with high proppant concentrations in the frac fluids or special ceramic proppants are required to stimulate flow in shales with low *BHN*. Ranges of values for BI_{min}, BI_{dyn} and *BHN* of North American prospective shales are taken from studies by Rickman et al. (2008), McKeon (2011), Sone and Zoback (2013), Yang et al. (2013). BI_{min}, BI_{dyn} and *BHN* values for the PSF are from Chesapeake (2010), sonic well logs (c.f. Eqs. (6)–(8)) and Bouw and Lutgert (2012), respectively. BI_{min}, BI_{dyn} and *BHN* values for the PSF are below or at the lower bound of values for the North American shales, indicating that PSF has relatively low brittleness and high tendency for proppant embedment.

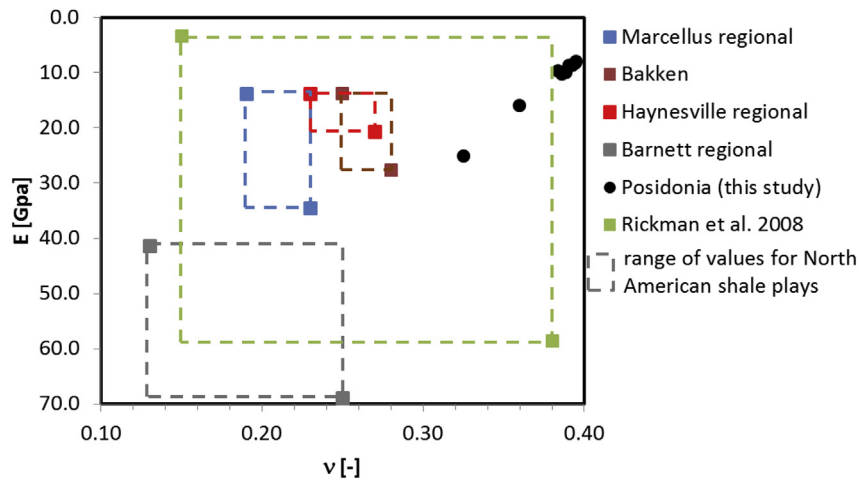

Fig. 8. Ranges of dynamic Young's modulus (E) and Poisson's ratio (ν) for the Marcellus Shale Formation, Bakken Formation, Haynesville Shale Formation and Barnett Shale Formation in North America and the Posidonia Shale Formation in the Netherlands.

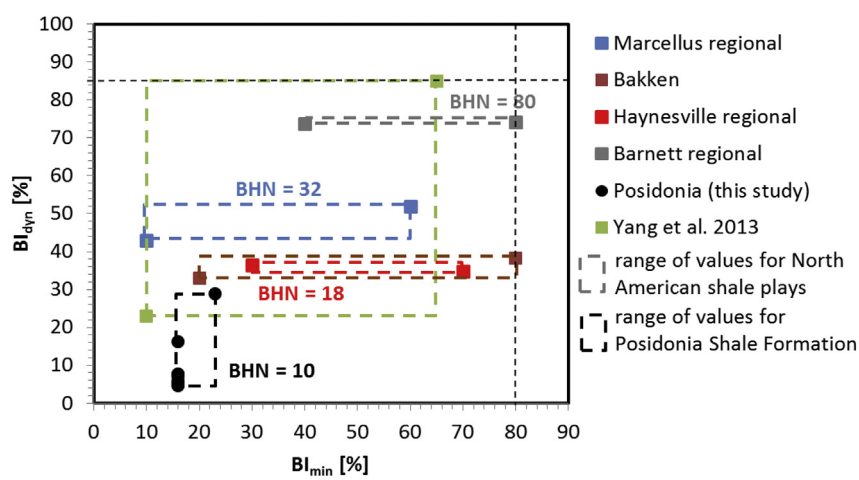

Fig. 9. Brittleness index based on mineralogy (BI_{min}, c.f. Eq. (10)), brittleness index based on dynamic elastic moduli (BI_{dyn}, c.f. Eq. (9)) and Brinell Hardness Number for the Marcellus Shale Formation, Bakken Formation, Haynesville Shale Formation and Barnett Shale Formation in North America and the Posidonia Shale Formation in the Netherlands. Note that for Posidonia wells where mineralogical data is absent, $BI_{min} = 16\%$ is assumed (i.e. the minimum value observed).

4.2. Key performance indicators

Performance indicators assessing the potential for hydrocarbon generation (PI_g), storage (PI_s) and flow stimulation (PI_f) are defined using maximum and minimum values for vitrinite reflectance (c.f. Fig. 6), total storage capacity for free and sorbed gas ($SC_{tot} = SC_f + SC_s$, c.f. Fig. 7), and brittleness index based on mineralogy and dynamic elastic moduli (Fig. 9)

$$PI_g = \frac{R_0 - R_0^{min}}{R_0^{max} - R_0^{min}} \tag{13}$$

$$PI_s = \frac{SC_{tot} - SC_{tot}^{min}}{SC_{tot}^{max} - SC_{tot}^{min}} \tag{14}$$

$$PI_f = \frac{1}{2}\left(\frac{BI_{min} - BI_{min}^{min}}{BI_{min}^{max} - BI_{min}^{min}} + \frac{BI_{dyn} - BI_{dyn}^{min}}{BI_{dyn}^{max} - BI_{dyn}^{min}}\right) \tag{15}$$

with R_o, SC_f, SC_s, BI_{min}, BI_{dyn} local values (based on well data) for the shale under investigation. Each performance indicator gas a value between 0 and 1 (or 0 and 100%) depending on the relative magnitude of the different shale properties compared to the range defined by prospective North American shales.

For example, if locally $R_o = 2.7$ then $PI_g = 100\%$, if $R_o = 1.0$ then $PI_g = 47\%$, and if $R_o = 0.55$ then $PI_g = 0\%$ (based on the current inventory of properties for North American shales yielding $R_o^{max} = 2.7$ and $R_o^{min} = 0.55$, c.f. Fig. 6). Note that minimum and maximum values for the different properties may be changed if more data becomes available (i.e. the performance indicators can be re-calibrated). In order to be able to map out shale prospectivity a mean performance indicator (PI_{mean}) is defined by the harmonic mean of PI_g, PI_s, PI_f

$$PI_{mean} = \frac{3}{PI_g^{-1} + PI_s^{-1} + PI_f^{-1}} \tag{16}$$

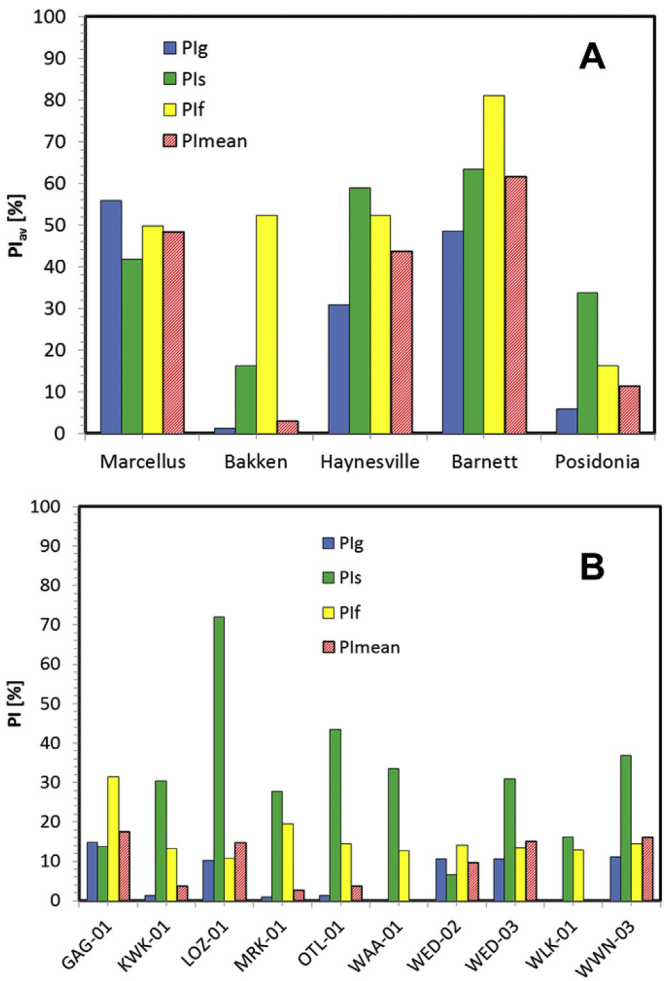

Fig. 10. Performance indicators for hydrocarbon generation (PI_g, in blue), storage (PI_s, in green) and flow stimulation (PI_f, in yellow) and the harmonic mean value (PI_{mean}) for different shales. (A) Performance indicators based on average values of regional shale properties for the Marcellus Shale Formation, Bakken Formation, Haynesville Shale Formation and Barnett Shale Formation in North America (c.f. Table 3) and the Posidonia Shale Formation (c.f. Table 2). (B) Local values of shale properties of the Posidonia Shale Formation at different well locations in the onshore part of the West Netherlands Basin (c.f. Fig. 1). (For interpretation of the references to colour in this figure legend, the reader is referred to the web version of this article.)

The choice for using a harmonic mean is motivated by the fact that this average augments the impact of low values for PI_g, PI_s, PI_f which means PI_{mean} is relatively low if one of the performance indicators is low. The use of a harmonic mean therefore agrees with the notion that potential for hydrocarbon generation, storage and flow stimulation all needs to be present for a shale to be prospective. As the relative importance of hydrocarbon generation, storage and flow stimulation in determining shale prospectivity is not well defined, PI_{mean} should be regarded as a qualitative empirical factor that indicates shale prospectivity on the basis of trends between shale properties and gas production observed in North American shales.

Calculation of the performance indicators for average (regional) properties of the North American shales shows how PI_g, PI_s, PI_f combine to PI_{mean} (Fig. 10). Except for the BF, all shales have a PI_{mean} above 40% with PI_{mean} highest in the BSF. PI_g and PI_s for the BF are much lower than for the other shales because it is in the oil window and the main reservoir is not a shale, but the Middle Member sandstone.

The performance indicators are well suited to indicate trends in local potential for hydrocarbon production at specific well locations. Performance indicators are calculated at different well locations across the PSF (Fig. 1). All well locations show reasonable potential for hydrocarbon storage (PI_s of 7–72%), but low potential for gas generation (PI_g of 1–15%) and flow stimulation (PI_f of 11–32%). Overall, PI_{mean} is lower than average PI_{mean} for North American shales (excluding the BF), indicating that the potential for gas production is at the lower bound of the North American potential. The limited overall potential for gas production is mainly due to limited potential for gas generation and flow stimulation. The potential for gas production is highest at wells GAG-01, WWN-03, WED-02, WED-03 and LOZ-01, and lowest or negligible at wells WAA-01, WLK-01, MRK-01, KWK-01 and OTL-01. If mapped at well locations, the performance indicators show that highest potential for gas production is at southern locations along the axis of the West Netherlands Basin where the PSF is at the largest depth and maturity is highest (Fig. 11). As maturity is the main limiting factor for gas production, locations with highest potential for gas production roughly coincide with locations with highest vitrinite reflectance (c.f. Figs. 4 and 10).

5. Implications for assessing the potential for hydrocarbon production in underexplored shales

It has been demonstrated how key performance indicators based on limited data can be used as empirical proxies for shale prospectivity and map out sweet spots in the Posidonia Shale Formation. Besides the use of the key performance indicators for sweet spot identification, it can also be attempted to assess potential correlations between performance indicators and resource estimates or well productivity using the inventory of North American shale properties. Moreover, a more detailed comparison of prospective North American shales and the level to which they can serve as analogues for the Posidonia Shale Formation can be made.

5.1. Correlation between performance indicators and hydrocarbon production

Direct correlation between local performance indicators and hydrocarbon production requires the full set of shale properties at specific well locations as well as local well productivity for North American shales. It is difficult to obtain these data from open literature (c.f. Table 3) as it requires proprietary data from North American operators. A direct link between the performance indicators and quantitative estimates of gas production is therefore difficult, but qualitative correlations can be made. Jarvie et al. (2007) link average gas flow from Barnett wells to vitrinite reflectance and mineralogy-based brittleness ($Q \sim \log R_o$, c.f. Fig. 6), which suggests PI_g and PI_f can be linked to gas production and used to extrapolate estimates of gas production if data from local wells becomes available. As GIP is linked to SC_{tot} and therefore to PI_s (c.f. Eq. (11)), uncertainties in resource estimates may be reduced if lateral variation of performance indicators is taken into account. PI_f is a proxy for brittleness that incorporates both mineralogy and elastic moduli. Therefore, PI_f may better predict the efficiency of flow stimulation than brittleness based on mineralogy or elastic moduli alone, and PI_f may correlate with local production gain due to hydraulic fracturing.

5.2. Comparison between the Posidonia Shale Formation and North American analogues to assess hydrocarbon production

The Posidonia Shale Formation can be characterized by (1) relatively low maturity (i.e. low PI_g, vitrinite reflectance similar to

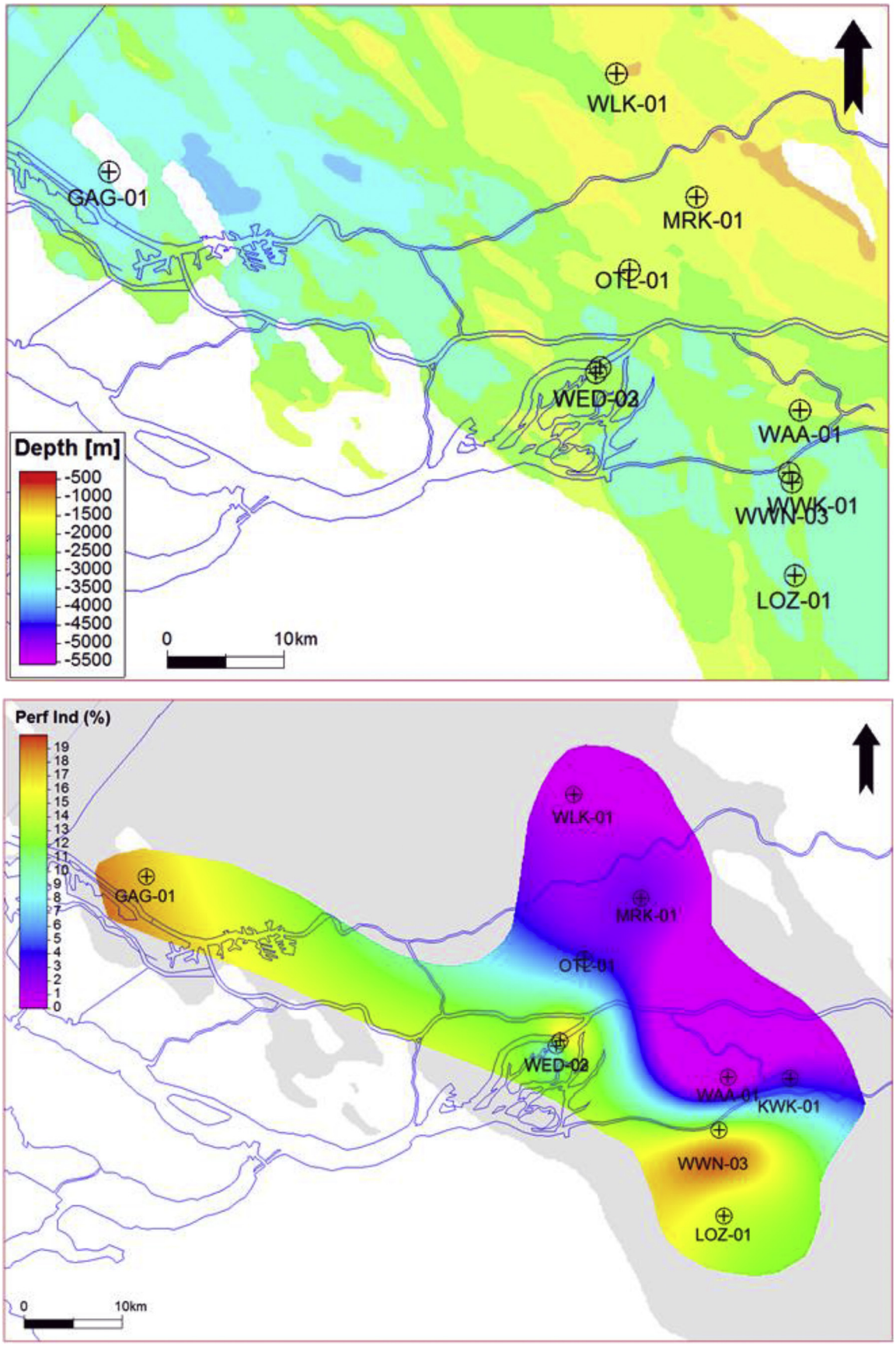

Fig. 11. Maps of depth distribution (top figure) and mean performance indicators (PI_{mean}, bottom figure, c.f. Eq. (16), Fig. 10) for the Posidonia Shale Formation at different well locations in the onshore part of the West Netherlands Basin.

oil-window thermal-maturity Barnett Shale, c.f. Figs. 2, 6 and 10) reasonable storage capacity (i.e. low to average PI_s, storage capacity for free and sorbed gas in the range of that of Marcellus and Haynesville, slightly lower than Barnett, c.f. Figs. 3, 7 and 10) low brittleness (i.e. low PI_s, brittleness lower than for North American shales, c.f. Figs. 9 and 10). In terms of maturity, the oil-window thermal-maturity Barnett Shale seems the best analogue. Ranges of depth, thickness, *TOC* and porosity also (partly) overlap (c.f. Tables 1–3). If similar well designs and stimulation efficiency as for Barnett wells can be implemented, gas flow may reach ~500 MCF/day (14 MCM/day, c.f. Fig. 6). However, the low brittleness of the Posidonia Shale Formation suggests that creep and proppant embedment may inhibit efficient flow stimulation (Ter Heege, 2014a). Upfront predictions of hydraulic fracture dimensions and gas production using conventional semi-analytical simulators suggest sustained gas flow rates over 10 years of production in the same range as for the Barnett (5–30 MCM/day, Godderij et al., 2014; Ter Heege, 2014b). These simulations yield cumulative gas production of 50–250 MMCM (mainly depending on well design and shale permeability, porosity and thickness) for 1 km horizontal wells with evenly spaced fractures. Maturity is also comparable to the Bakken shales, which have generated oil and gas in the neighbouring sandstone (Middle Member) reservoir. Besides ~600 BBL/day of oil, new-well gas production per rig for the Bakken is ~600 MCM/day (Table 3, EIA, 2015a,b). Accordingly, the PSF could produce oil from nearby sandy formations or intervals, if present. However, low brittleness, shale creep and proppant embedment in the PSF may hamper hydrocarbon production. The Marcellus and Haynesville shales are more mature than the Posidonia Shale Formation and therefore have a larger potential for gas production.

5.3. Potential for application to underexplored shales worldwide

In general, sweet spot identification in shales is based on finding optimum combinations of properties (e.g., Wang and Gale, 2009; McKeon, 2011). Although performance indicators are applied to the Posidonia Shale Formation in this study, a similar approach can be applied to underexplored shales elsewhere in the world. The main added value of using the performance indicators is that they can be used to indicate shale prospectivity on the basis of a few key properties that can be readily assessed using limited available data. In addition, local trends in hydrocarbon potential can be mapped if well data at different location in a shale basin is available. The mean performance indicator can be used to assess preferential sites to initiate exploratory drilling in virgin shale basins.

The mean performance indicator can be used to rank the prospectivity shale relative to the hydrocarbon producing shales in North America. As shown in section 5.2, the performance indicator assessing the potential for hydrocarbon generation can be used to assess shale maturity and to provide a first estimate of potential gas flow rates by comparison with prospective North American shales (Jarvie et al., 2007). The performance indicator assessing the potential for hydrocarbon storage can be used to improve resource estimates and to provide a first estimate of typical cumulative gas production that can be attained (EIA, 2011, 2015a,b). The performance indicator assessing the potential for flow stimulation can be used to better assess brittleness and help optimizing the design of hydraulic fracturing operations (King, 2010; McKeon, 2011). In general, mapping of key performance indicators aid in optimizing field development planning for virgin shale basins targeted for hydrocarbon exploitation.

6. Summary & conclusions

A key performance indicator has been defined that describe the potential of hydrocarbon production across underexplored shale basins on the basis of a limited number of local properties of shales. The indicator combines three performance indicators that describe the potential for hydrocarbon generation, storage capacity, and flow stimulation. Hydrocarbon generation potential (maturity) is described using vitrinite reflectance, storage capacity potential for free and sorbed gas is described using depth, thickness, porosity and the volume of sorbed methane per volume of shale, and flow stimulation potential is described using brittleness based on mineralogy and dynamic elastic moduli. The indicators are benchmarked using properties of prospective North American shales (Marcellus, Bakken, Haynesville and Barnett), and applied to the Posidonia Shale Formation in the Netherlands. Performance indicators for North American shales can be cross-compared to other shales to indicate potential for hydrocarbon production, and mapped out to determine sweet spots in shale basins. It can be concluded that:

- Average performance indicators for the Marcellus, Bakken, Haynesville, Barnett and Posidonia are 48%, 3%, 44%, 62% and 12%, respectively (i.e. the theoretical maximum is 100%). Performance indicators for North American shales follow known trends of shale prospectivity within shale basins. Values are lower for the Posidonia than for the North American Shales, mainly due to low maturity and brittleness. The low performance indicator for flow stimulation ("brittleness") for the Posidonia Shale Formation suggests that creep and proppant embedment may inhibit efficient flow stimulation
- Mapping of the mean performance indicator in the study area shows that the highest potential for gas production in the Posidonia Shale Formation is at southern locations along the axis of the West Netherlands Basin with local maxima around wells WWN-03 ($PI_{mean} = 16\%$) and GAG-01 ($PI_{mean} = 18\%$). Maximum values of the mean performance indicator correlate with local maxima in vitrinite reflectance and depth. At the location of well LOZ-01 the potential for hydrocarbon storage is highest, but the potential for flow stimulation is lowest.
- Oil-window thermal-maturity Barnett Shale shows similar potential for hydrocarbon generation, slightly higher hydrocarbon storage potential and much higher potential for flow stimulation. Wells in the Barnett areas that are in oil-window thermal-maturity areas reach average gas flow of ~500 MCF/day (14 MCM/day), which is in rough agreement with upfront predictions of hydraulic fracture dimensions and gas production in the Posidonia Shale Formation.
- Comparison with other North American shales shows that maturity is comparable to that of Bakken shales, but lower than that of the Marcellus and Haynesville shales. New-well hydrocarbon production per rig for the Bakken is ~600 BBL/day of oil and ~600 MCM/day of gas, which suggest oil and gas production should be considered for the Posidonia shale formation.
- If mapping of key performance indicators is applied to underexplored shales, local sweet spots can be better identified upfront, before large scale exploitation has commenced. Therefore, it aids in locating preferential sites to initiate exploratory drilling and in optimizing field development planning.

Acknowledgements

The authors wish to acknowledge the early work by Frank van Bergen on data used in the present study as well as discussions on shale plays in the Netherlands. Martyn Drury (Utrecht University) assisted in obtaining the FIB-SEM image (Fig. 2E).

Appendix A

Table A.1
Abbreviations and definitions of symbols used in the paper. Where available references for application to the Posidonia Shale Formation (PSF-*reference*) are given rather than general references.

Abbreviation	Definition	Reference/comment
symbols [unit]		
A [m^2]	Area of shale	Table 1
B [sm^3/m^3]	Volume factor- gas (B_g) or oil formation gas volume factor (B_{oi})	$B = 1/F_{expZ}$ (EIA, 2011)
BHN	Brinell hardness number	PSF-Bouw and Lutgert 2012
BI	Brittleness index- based on dynamic elastic moduli (BI_{dyn}) or	Eq. (9); Tables 2 and 3 (Rickman et al., 2008)
	Mineralogical composition (BI_{min})	Eq. (10); Tables 2 and 3 (Jarvie et al., 2007)
Ca [wt%]	Carbonate content	Eq. 10
Cl [wt%]	Clay content	Eq. 10
E_{dyn} [GPa]	Dynamic Young's modulus	Eq. (6); Table 2 (Fjaer et al., 2008)
EUR [m^3 or ft^3]	Estimated ultimate recovery	Table 2
F_{expZ} [sm^3/m^3]	Depth-dependent expansion factor for hydrocarbons	Eq. 11
GIP [m^3 or ft^3]	Gas in place	Table 3 (EIA, 2011)
LOM	Level of organic metamorphism	Eq. (1) (Hood et al., 1975)
OIP [barrels]	Oil in place	Table 3 (EIA, 2011)
PI [%]	Performance Indicator- hydrocarbon generation (PI_g), storage (PI_s),	Eqs. (13)–(16)
	flow stimulation (PI_f) or mean (PI_{mean})	
Q [m^3 or ft^3]	Gas production- cumulative production (Q_{cum}) or Flow rate (Q_{well})	Table 3
Qz [wt%]	Quartz content	Eq. 10
R_o [%]	Vitrinite reflectance	Tables 2 and 3; Fig. 4
S [%]	Saturation- gas (S_{gT}), oil (S_{oT}), or water (S_{wT}) saturation of total porosity	Table 1, Eq. 3
SC	Storage capacity- total (SC_{tot}), free gas (SC_f) or sorbed gas (SC_s)	Eqs. (11) and (12); Fig. 7
TOC [wt%]	Total organic carbon	Eq. (4) and (5); Tables 2 and 3
v [km/s]	Sonic wave velocity- compressional (v_p) or shear (v_s) sonic wave	Eqs. (6)–(8)
V [m^3 or ft^3]	Volume- total (V_{tCH4}), free (V_{fCH4}) or Sorbed (V_{sCH4}) methane, rock (V_r)	Table 1, Eq. 12
Z [m]	True vertical depth	Tables 2 and 3
Δz [m]	Formation thickness	Tables 2 and 3
ϕ [%]	Porosity- total (ϕ_{tot}) or Hydrocarbon-filled (ϕ_{hc})	Eq. (3) and (5); Tables 2 and 3
κ [mD]	Permeability	Table 3
ρ [g/cm^3]	Density- bulk shale (ρ_{bulk}, ρ_b), solid constituents (ρ_{solid}), non-hydrocarbon	Eqs. (3)–(6)
	pore fluid (ρ_f), hydrocarbons (ρ_{hc}), shale matrix (ρ_{mat}) or organic matter (ρ_{TOC})	
ν_{dyn}	Dynamic Poisson's ratio	Eq. (7); Table 2
Well logs [unit]		
GR [API]	Gamma ray	Fig. 3
DT [μs/ft]	Compressional sonic travel time	Eq. (2); Fig. 3
DT_{BASE} [μs/ft]	Sonic baseline (scaled)	Eq. 2
MD [m]	Measured depth	Fig. 3
RESD [ohm m]	Deep resistivity	Eq. 2
$RESD_{BASE}$ [ohm.m]	Deep resistivity baseline (scaled)	Eq. 2
RHOB [g/cm^3]	Bulk density	Fig. 3
TOC_{LD} [wt%]	Log-derived total organic carbon	Eq. (1); Fig. 3 (Passey et al., 1990)
ΔlogR	Curve separation resistivity and compressional sonic logs	Eq. (1) and (2); Fig. 3 (Passey et al., 1990)
Formations		
BF	Bakken formation	Williston basin, North Dakota (Fig. 5)
BSF	Barnett shale formation	Fort Worth basin, Texas
HSF	Haynesville shale formation	Northwest Louisiana (Fig. 5)
MSF	Marcellus shale formation	Appalachian basin (Fig. 5)
PSF	Posidonia shale formation	West Netherlands basin (Fig. 1)
Posidonia wells		
GAG-01	Gaag-01 (NAM, 1971)	Table 2, www.nlog.nl
KWK-01	Kerkwijk-01 (NAM, 1988)	Table 2, www.nlog.nl
LOZ-01	Loon op Zand-01 (NAM, 1952)	Table 2, www.nlog.nl
MRK-01	Meerkerk-01 (NAM, 1989)	Table 2, www.nlog.nl
OTL-01	Ottoland-01 (NAM, 1988)	Table 2, www.nlog.nl
WAA-01	Wijk-Aalburg-01 (NAM, 1972)	Table 2, www.nlog.nl
WED-02/03	Werkendam-02/03 (NAM, 1965)	Table 2, www.nlog.nl
WLK-01	Willeskop-01 (NAM, 1988)	Table 2, www.nlog.nl
WWN-03	Waalwijk Noord-03 (Clyde, 1998)	Table 2, www.nlog.nl
Analysis methods		
FIB-SEM	Focused ion beam scanning electron microscopy	PSF-Verreussel et al., 2013,
		Houben et al., 2014
NMR	Nuclear magnetic resonance (porosity, TOC)	Jacobi et al., 2009
Permeability-GRI	Permeability measurement following method of Gas Research Institute	PSF-Bouw and Lutgert 2012
Permeability-GRI	Permeability measurement using pulse decay method	PSF-Bouw and Lutgert 2012
Rock-Eval	Pyrolysis method (TOC)	PSF-Van Bergen et al., 2013
$\delta^{13}C_{org}$	Ratio of carbon isotopes $^{13}C/^{12}C$	PSF-Verreussel et al., 2013
Gas volume units		
MCM	1000 m^3 (35.31 MCF)	Thousand cubic meter
MMCM	1000000 m^3 (35.31 MMCF)	Million cubic meter
BCM	1000000000 m^3 (35.31 BCF)	Billion cubic meter
MCF	1000 ft^3 (28.32 CM)	Thousand cubic feet

(*continued on next page*)

Table A.1 (*continued*)

Abbreviation	Definition	Reference/comment
MMCF	1000000 ft^3 (28.32 MCM)	Million cubic feet
BCF	10000000 ft^3 (28.32 MMCM)	Billion cubic feet
TCF	1000000000 ft^3 (28.32 BCM)	Trillion cubic feet
Oil volume units		
BBL	Barrels	
MBBL	1000 barrels	Thousand barrels

References

Bernard, S., Horsfield, B., Schulz, H.-M., Wirth, R., Schreiber, A., Sherwood, N., 2012. Geochemical evolution of organic-rich shales with increasing maturity: a STXM and TEM study of the Posidonia Shale (Lower Toarcian, northern Germany). Mar. Petroleum Geol. 31, 70–89.

Bouw, S.S., Lutgert, J., 2012. Shale Plays in the Netherlands. SPE 152644.

Bowker, K.A., 2007. Development of the Haynesville shale play, Fort Worth Basin. AAPG Bull. 91.

Browning, J., Ikonnikova, S., Gülen, G., Tinker, S., 2013. Barnett Shale Production Outlook. Society of Petroleum Engineers. http://dx.doi.org/10.2118/165585-PA.

Bust, V.K., Majid, A.A., Oletu, J.U., Worthington, P.F., 2013. The petrophysics of shale gas reservoirs: technical challenges and pragmatic solutions. Pet. Geosci. 19, 91–103.

Carter, K.M., Harper, J.A., Schmid, K.W., Kostelnik, J., 2011. Unconventional natural gas resources in Pennsylvania: the backstory of the modern Marcellus shale play. Environ. Geosci. 18, 217–257.

Castagna, J.P., Batzle, M.L., Eastwood, R.L., 1985. Relationships between compressional-wave and shear-wave velocities in elastic silicate rocks. Geophysics 50, 571–581.

Charpentier, R.R., Cook, T.A., 2010. Improved USGS Methodology for Assessing Continuous Petroleum Resources, Version 2: U.S. In: Geological Survey Data Series, 547, p. 22 and program. Revised November 2012.

Charpentier, R.R., Cook, T.A., 2013. Variability of Oil and Gas Well Productivities for Continuous (Unconventional) Petroleum Accumulations: U.S. Geological Survey Open-File Report 2013–1001, 3 sheets.

Chesapeake, 2010. Posidonia Project Cuttings Research. Report. www.nlog.nl.

Crain, E.R., Holgate, D., 2014. A 12-Step program to reduce uncertainty in Kerogen-rich reservoirs. In: CSPG-CSEG-CWLS Geo Convention 2014: Focus. Calgary, Canada, p. 11.

De Jager, J., Doyle, M.A., Grantham, P.J., Mabillard, J.E., 1996. Hydrocarbon habitat of the west Netherlands Basin. In: Rondeel, H.E., Batjes, D.A.J., Nieuwenhuis, W.H. (Eds.), Geology of Gas and Oil under the Netherlands Dordrecht, Kluwer/KNGMG, pp. 191–209.

De Jager, J., Geluk, M.C., 2007. Petroleum geology. In: Wong, T.E., Batjes, D.A.J., De Jager, J. (Eds.), Geology of the Netherlands. Royal Dutch Academy of Arts and Sciences, Amsterdam, pp. 237–260.

Economides, M.J., Nolte, K.G., 2000. Reservoir Stimulation, third ed. John Wiley and Sons, London.

EIA, 2011. Review of Emerging Resources: U.S. Shale Gas and Shale Oil Plays. U.S. Energy Information Administration. www.eia.gov.

EIA, 2015a. Annual Energy Outlook 2015 with Projections to 2040. U.S. Energy Information Administration. www.eia.gov.

EIA, 2015b. Drilling Productivity Reports: Marcellus Region, Bakken Region, Haynesville Region. U.S. Energy Information Administration. www.eia.gov.

Eissa, E.A., Kazi, A., 1988. Relation between static and dynamic Young's Moduli of rocks. Int. J. Rock Mech. Min. Sci. Geomech. Abstr 25, 479–482.

Fjaer, E., Holt, R.M., Horsrud, P., Raaen, A.M., Risnes, R., 2008. Petroleum Related Rock Mechanics In: Developments in Petroleum Science, second ed., 52. Elsevier, Amsterdam.

Frimmel, A., Oschmann, W., Schwark, L., 2004. Chemostratigraphy of the Posidonia Black Shale. SW Germany. Influence of sea-level variation on organic facies evolution. Chem. Geol. 206, 199–230.

Gargouri, M., 2012. Multicomponent 3D Seismic Interpretation of the Marcellus Shale Bradford County, Pennsylvania. Ph. D. thesis. University of Houston.

Gasparik, M., Ghanizadeh, A., Bertier, P., Gensterblum, Y., Bouw, S., Krooss, B.M., 2012. High-pressure methane sorption isotherms of black shales from The Netherlands. Energy & Fuels 26, 4995–5004.

Godderij, R., Brouwer, B., Harings, M., Scheffers, B.C., Brolsma, M.-J., Bouw, S., 2014. A Conceptual Shale Gas Field Development Plan for the Lower Jurassic Posidonia Shale in The Netherlands. Society of Petroleum Engineers. http://dx.doi.org/10.2118/167796-MS.

Hammes, U., Hamlin, H.S., Ewing, T.E., 2011. Geologic analysis of the Upper Jurassic Haynesville shale in East Texas and West Louisiana. AAPG Bull. 95, 1643–1666.

Hammes, U., Frebourg, G., 2012. Haynesville and Bossier mudrocks: a facies and sequence stratigraphic investigation, East Texas and Louisiana, USA. Mar. Petroleum Geol. 31, 8–26.

Hartwig, A., Schulz, H.-M., 2010. Applying classical shale gas evaluation concepts to Germany-Part I: the basin and slope deposits of the Stassfurt Carbonate (Ca2, Zechstein, Upper Permian) in Brandenburg. From Visions to Solutions 70, Supplement 3 Chem. Erde – Geochem. Geoenergy 77–91.

Heller, R., Zoback, M., 2014. Adsorption of methane and carbon dioxide on gas shale and pure mineral samples. J. Unconv. Oil Gas Resour. 8, 14–24.

Herber, R., De Jager, R., 2010. Oil and gas in the Netherlands – is there a future? Neth. J. Geosciences – Geol. en Mijnbouw 89–2, 119–135.

Hesselbo, S.P., Pieńkowski, G., 2011. Stepwise atmospheric carbon-isotope excursion during the Toarcian oceanic anoxic event (Early Jurassic, Polish Basin). Earth Planet. Sci. Lett. 301, 365–372.

Hood, A., Gutjahr, C.M., Heacock, R.L., 1975. Organic metamorphism and the generation of petroleum. AAPG Bull. 59, 986–996.

Houben, M.E., Barnhoorn, A., Drury, M.R., Peach, C.J., Spiers, C.J., 2014. Microstructural investigation of the Whitby mudstone (UK) as an analog for Posidonia Shale (NL). In: 76th European Association of Geoscientists and Engineers Conference and Exhibition 2014 – Experience the Energy, Amsterdam, The Netherlands. European Association of Geoscientists and Engineers (EAGE).

Jacobi, D.J., Breig, J.J., LeCompte, B., Kopal, M., Hursan, G., Mendez, F.E., Bliven, S., Longo, J., 2009. Effective geochemical and geomechanical characterization of shale gas reservoirs from the wellbore environment: Caney and the Woodford shale. In: SPE Annual Technical Conference and Exhibition, New Orleans, Louisiana, 4–7 October. Society of Petroleum Engineers. SPE-124231-MS.

Jarvie, D.M., Hill, R.J., Ruble, T.E., Pollastro, R.M., 2007. Unconventional shale-gas systems: the Mississippian Barnett Shale of north-central Texas as one model for thermogenic shale-gas assessment. Am. Assoc. Petroleum Geol. Bull. 91, 475–499.

Jarvie, D.M., Coskey, R.J., Johnson, M.S., Leonard, J.E., 2011. The Geology and Geochemistry of the Parshall Area, Mountrail County, North Dakota.

Kaiser, M.J., Yu, Y., 2011. Haynesville shale well performance and development potential. Nat. Resour. Res. 20, 217–229.

Kaiser, M.J., Yu, Y., 2013. Haynessville update-1: North Louisiana gas shale's drilling decline precipitous. Oil Gas J. 111.

King, G.E., 2010. Thirty Years of Gas Shale Fracturing: what Have We Learned? SPE 133456.

Langmuir, I., 1918. The adsorption of gases on plane surfaces of glass, mica and platinum. J. Am. Chem. Soc. 40, 1361–1403.

Lee, D.S., Herman, J.D., Elsworth, D., Kim, H.T., Lee, H.S., 2011. A critical evaluation of unconventional gas recovery from the Haynesville shale, Northeastern United States. KSCE J. Civ. Eng. 15, 679–687.

Lemmon, E.W., McLinden, M.O., Friend, D.G., 2011. Thermophysical properties of fluid systems. In: Linstrom, P.J., Mallard, W.G. (Eds.), NIST Chemistry WebBook. NIST Standard Reference Database Number 69, National Institute of Standards and Technology. Gaithersburg MD, 20899. http://webbook.nist.gov (retrieved June, 2015).

Lott, G.K., Wong, T.E., Dusar, M., Andsbjerg, J., Mönnig, E., Feldman- Olszewska, A., Verreussel, R.M.C.H., 2010. Jurassic. In: Doornenbal, J.C., Stevenson, A.G. (Eds.), Petroleum Geological Atlas of the Southern Permian Basin Area. EAGE Publications, Houten, pp. 175–193.

McArthur, J.M., Algeo, T.J., Van de Schootbrugge, B., Li, Q., Howarth, R.J., 2008. Basinal restriction, black shales, Re-Os dating, and the Early Toarcian (Jurassic) oceanic anoxic event. Paleoceanography 23. http://dx.doi.org/10.1029/2008PA001607.

McKeon, 2011. Horizontal Fracturing in Shale Plays. Halliburton. www.thepttc.org/workshops/eastern_062111/eastern_062111_McKeon.pdf.

Milici, R.C., Swezey, C., 2006. Assessment of Haynesville Basin Oil and Gas Resources: Devonian Shale-middle and Upper Haynesville Total Petroleum System. US Department of the Interior, US Geological Survey.

Montgomery, S.L., Jarvie, D.M., Bowker, K.A., Pollastro, R.M., 2005. Mississippian Barnett shale, fort Worth Basin, North-Central Texas: gas-shale play with multi-trillion cubic foot potential. AAPG Bull. 89, 155–175.

Nelskamp, S., Verweij, J.M., 2012. Using Basin Modeling for Geothermal Energy Exploration in the Netherlands – an Example from the West Netherlands Basin and Roer Valley Graben. TNO report, TNO-060-UT-2012–00245, Utrecht, p. 113. www.nlog.nl/resources/Publicaties/TNO-060-UT-2012-00245.pdf.

Nunn, J.A., 2012. Burial and thermal history of the Haynesville shale: implications for overpressure, gas generation, and natural hydrofracture. GCAGS J. 1, 81–96.

Parker, M.A., Buller, D., Petre, J.E., Dreher, D.T., et al., 2009. Haynesville shale-petrophysical evaluation. In: SPE Rocky Mountain Petroleum Technology Conference. Society of Petroleum Engineers.

Passey, Q.R., Creaney, S., Kulla, J.B., Moretti, F.J., Stromi, J.D., 1990. A practical model for organic richness from porosity and resistivity logs. AAPG Bull. 74, 1777–1794.

Passey, Q.R., Bohacs, K., Esch, W.L., Klimentidis, R., Sinha, S., 2010. From Oil-prone Source Rock to Gas-Producing Shale Reservoir – Geologic and Petrophysical Characterization of Unconventional Shale Gas Reservoirs. Society of Petroleum

Engineers. http://dx.doi.org/10.2118/131350-MS.
Pitman, J.K., Price, L.C., LeFever, J.A., 2001. Diagenesis and Fracture Development in the Bakken Formation, Williston Basin: Implications for Reservoir Quality in the Middle Member.
Ramurthy, M., Barree, R.D., Kundert, D.P., Petre, J.E., Mullen, M.J., 2011. Surface-area Vs. Conductivity-type Fracture Treatments in Shale Reservoirs. Society of Petroleum Engineers. http://dx.doi.org/10.2118/140169-PA.
Rickman, R., Mullen, M.J., Petre, J.E., Grieser, W.V., Kundert, D., 2008. A Practical Use of Shale Petrophysics for Stimulation Design Optimization: All Shale Plays Are Not Clones of the Barnett Shale. Society of Petroleum Engineers.
Röhl, H.J., Schmid-Röhl, A., Oschmann, W., Frimmel, A., Schwark, L., 2001. The Posidonia Shale (Lower Toarcian) of SW-Germany: an oxygen-depleted ecosystem controlled by sea level and palaeoclimate. Palaeogeogr. Palaeoclimatol. Palaeoecol. 165, 27–52.
Sondergeld, C.H., Newsham, K.E., Comisky, J.T., Rice, M.C., Rai, C.S., 2010. Petrophysical Considerations in Evaluating and Producing Shale Gas Resources. Society of Petroleum Engineers. http://dx.doi.org/10.2118/131768-MS.
Sone, H., Zoback, M., et al., 2010. Strength, creep and frictional properties of gas shale reservoir rocks. In: 44th US Rock Mechanics Symposium and 5th US-Canada Rock Mechanics Symposium. American Rock Mechanics Association.
Sone, H., Zoback, M.D., 2013. Mechanical properties of shale-gas reservoir rocks – Part 1: static and dynamic elastic properties and anisotropy. Geophysics 78, D381–D392.
Sorensen, J.A., Terneus, J.R., 2008. Evaluation of Key Factors Affecting Successful Oil Production in the Bakken Formation, North Dakota. Technology Status Assessment. Energy and Environmental Research Center, Grand Forks, ND (Report submitted to US Department of Energy).
Suan, G., Pittet, B., Bour, I., Mattioli, E., Duarte, L.V., Mailliot, S., 2008. Duration of the early Toarcian carbon isotope excursion deduced from spectral analysis: consequence for its possible causes. Earth Planet. Sci. Lett. 267, 666–679.
Ter Heege, J.H., Zijp, M., De Bruin, G., Buijze, L., 2014a. Upfront Predictions of Hydraulic Fracturing and Gas Production in Underexplored Shale Gas Basins: Example of the Posidonia Shale Formation in the Netherlands. In: 48th US Rock Mechanics/Geomechanics Symposium, 1–4 June, Minneapolis, MN. ARMA-2014-7205.
Ter Heege, J.H., Zijp, M.H.A.A., De Bruin, G., Ten Veen, J.H., 2014b. Addressing uncertainties in estimates of recoverable gas for underexplored shale gas basins. In: Second EAGE/SPE/AAPG Shale Gas Workshop in the Middle East, Dubai, UAE, 21 September 2014, EAGE.
Trabucho-Alexandre, A., Dirkx, R., Veld, H., Klaver, G., de Boer, P.L., 2012. Toarcian black shales in the Dutch Central Graben; record of energetic, variable depositional conditions during an oceanic anoxic event. J. Sediment. Res. 82, 104–120.
Van Balen, R.T., Van Bergen, F., De Leeuw, C., Pagnier, H., Simmelink, H., Van Wees, J.D., Verweij, J.M., 2000. Modelling the hydrocarbon generation and migration in the West Netherlands Basin, the Netherlands. Geol. en Netherl. J. Geosci. 79, 29–44.
Van Bergen, F., Zijp, M.H.A.A., Nelskamp, S., Kombrink, H., 2013. Shale gas evaluation of the early jurassic posidonia shale formation and the carboniferous Epen formation in the Netherlands. AAPG Hedb. Mem. 103, 1–24.
Verreussel, R.M.C.H., Zijp, M.H.A.A., Nelskamp, S., Wasch, L., de Bruin, G., Ter Heege, J., Ten Veen, J.H., 2013. Pay-zone Identification Workflow for Shale Gas in the Posidonia Shale Formation, the Netherlands, First Break vol. 31.
Wang, F.P., Gale, J.F., 2009. Screening criteria for shale-gas systems. Gulf Coast Assoc. Geol. Soc. Trans. 59, 779–793.
Webster, R.L., 1984. Petroleum Source Rocks and Stratigraphy of the Bakken Formation in North Dakota.
Wrightstone, G., 2009. Marcellus shale: geologic controls on production. In: American Association of Petroleum Geologists Annual Convention, Denver CO, June.
Yang, Y., Sone, H., Hows, A., Zoback, M.D., 2013. Comparison of brittleness indices in organic-rich shale formations. In: 47th U.S. Rock Mechanics/Geomechanics Symposium, San Francisco, California, 23–26 June. American Rock Mechanics Association ARMA-2013-403.
Zijp, M.H.A.A., Nelskamp, S., Schavemaker, Y.A., ten Veen, J.H., ter Heege, J.H., 2013. Multidisciplinary Approach for Detailed Characterization of Shale Gas Reservoirs, a Netherlands Showcase, OTC-24383-MS.
Zijp, M.H.A.A., Ter Heege, J.H., 2014. Shale gas in the Netherlands: current state of play. Int. Shale Gas Oil J. 2, 59–63.
Zijp, M.H.A.A., Ten Veen, J.H., Verreussel, R., Ter Heege, J.H., Ventra, D., Martin, J., 2015. Shale Gas Formation Research: from Well Logs to Outcrop – and Back Again, First Break vol. 33.